

Evaluation of Flow Rate and Leakage on Mask Effectiveness and Investigation of Double Masks

Thesis by
Peter Chea

In Partial Fulfillment of the Requirements for the
Degree of
Bachelor of Science in Chemical Engineering

The logo for the California Institute of Technology (Caltech), featuring the word "Caltech" in a bold, orange, sans-serif font.

CALIFORNIA INSTITUTE OF TECHNOLOGY
Pasadena, California

2022
Final Edits made July 2024

© 2022

Peter Chea

ORCID: 0009-0005-0774-6715

All rights reserved

ACKNOWLEDGEMENTS

I would like to thank my postdoc Buddhi Pushpawela for her guidance and hard work during my thesis. She was the primary person I would look towards for guidance when there seemed like there was no direction for the project. She did a significant amount of the mask testing and data analysis since I could only come to the lab once a week with the COVID restrictions, and I am sincerely grateful for these efforts. I thank her for recommending relevant papers and critiquing this thesis. She told me her experiences from graduate school, and it inspired me to apply for graduate school because of her passion and curiosity.

I would like to thank Richard Flagan for allowing me to remain involved with the lab since he took me in as a confused freshman. Rick's knowledge on aerosols and how he explains the science behind the various concepts we discussed was simply amazing to me. I had the opportunity to work with excellent minds from JPL the summer after my freshman year testing air quality sensors. The knowledge, advice, and skills that I accumulated in this lab have led me to realize that the environmental field, specifically air quality, is a desirable yet attainable path.

Oddly, I would like to thank this historical period of 2020-2021. With remote learning due to COVID-19, I still can never get used to lectures on zoom and the lack of social interactions that we would usually have on campus. Yet, because of this pandemic, while I was trying to find something to do for summer, Rick said I could research about modelling a hospital room and tracking the concentration of virus. This summer work transformed into this thesis investigating the effectiveness of masks. This period of time was strange, but it has brought an excellent opportunity for me.

For my entire research career, I would like to thank the other members of the Flagan lab that I worked with, specifically Stephanie Kong, Ryan Ward, Stavros Amanatidis; they provided lots of support and advice during my time in the lab. The humor of these individuals has truly humored me in my path to becoming a better researcher.

Lastly, I would like to thank my friends and family for supporting me through this thesis and also through my Caltech journey.

ABSTRACT

Mask-wearing emerged as the primary safety measure to prevent spreading COVID-19. To assess the viability of different materials in filtering aerosols when inhaling, we tested multiple copies of different mask categories: including NIOSH-certified N95 respirators, KN95 respirators, procedure masks, and cloth masks. The intact masks were exposed to polydisperse NaCl aerosol of 30-800 nm, and tightly sealed within a chamber to get the upstream and downstream particle counts and pressure measurements. The pressure drop was measured for seven flow rates between 5 and 85 LPM. For all masks, it increased linearly with flow rate with $r^2 > 0.98$. The KN95 and cloth masks had higher pressure drops than the other masks, causing reduced breathability. The penetration was calculated with counts from a differential mobility analyzer and condensation particle counter system for three flow rates: 5, 30, and 85 LPM. For all of the masks, the penetration increased with flow rate, while the most penetrating particle size (MPPS) generally decreased. The peak penetration is lowest for N95 respirators, and the peak penetration is highest for cloth masks at all flow rates. The use of face masks at high flow rates increases the risk to the wearer, and reduces breathability. All double mask combinations tested had lower penetration values and higher pressure drops than a corresponding single mask. The data obtained indicate that wearing combinations of cloth and procedure masks are similar to wearing an N95 respirator and better than the tested KN95 respirator in terms of maximum penetration. We observe that wearing a combination of cloth and procedure masks has a higher amount of decreased penetration and a lower amount of increased pressure drop than a combination involving N95 and KN95 respirators. For the resistance of leakage, a parallel resistance model was used to calculate the resistance for leaks. The primary assumption was that particles could only flow through the mask into the mouth or through leakages in the nasal and cheek areas. For leakage flow rate, the pressure drop data from a material test without leaks and mannequin test with some leakage were utilized. With the mannequin test, the chamber was equipped with a mannequin head with pipes inside to connect the opening from the mouth and the bottom of the neck in order to evaluate the fit of masks on human faces. The procedure and cloth masks had lower resistance for leaks and leakage flow rates than N95 and KN95 respirators. The procedure and cloth masks are more susceptible to leaks than respirators and thus reducing the effectiveness of these masks.

PUBLISHED CONTENT AND CONTRIBUTIONS

Chea, P. H., Pushpawela, B., Ward, R. X., & Flagan, R. C. (2024). Is double masking even worthwhile? *Aerosol Science and Technology*, 58(9), 965–977. <https://doi.org/10.1080/02786826.2024.2369638>

P.H.C. assisted with preparing the experimental setup, conducted the experiments, analyzed the data, wrote the first draft of the manuscript, and edited the manuscript.

Pushpawela, B., Chea, P. H., Ward, R. X., & Flagan, R. C. (2023). Quantification of face seal leakage using parallel resistance model. *Physics of Fluids*, 35(12). <https://doi.org/10.1063/5.0177717>

P.H.C. assisted with preparing the experimental setup, conducted the experiments, analyzed the data, and edited the manuscript.

TABLE OF CONTENTS

| | |
|--|------|
| Acknowledgements | iii |
| Abstract | iv |
| Published Content and Contributions | v |
| Table of Contents | v |
| List of Illustrations | vii |
| List of Tables | viii |
| Chapter I: Introduction | 1 |
| Chapter II: Materials and Methods | 6 |
| 2.1 Masks | 6 |
| 2.2 Experimental Setup and Procedure | 6 |
| 2.3 Mask performance metrics | 9 |
| 2.4 Data Analysis | 9 |
| Chapter III: Single Mask Results | 11 |
| 3.1 Pressure Drop | 11 |
| 3.2 Penetration | 13 |
| Chapter IV: Double Mask Results | 18 |
| 4.1 Experimental Reasoning | 18 |
| 4.2 Pressure Drop | 19 |
| 4.3 Penetration | 20 |
| Chapter V: Measures to Quantify Leakage | 24 |
| 5.1 Resistance of Leaks | 24 |
| 5.2 Flow Rate of Leaks | 25 |
| Chapter VI: Discussion and Future Work | 29 |
| Bibliography | 33 |
| Appendix A: Specification of Masks | 38 |
| Appendix B: Linear Plots of Penetration for Double Masks | 39 |
| Appendix C: Updates to this Thesis in 2024 | 41 |
| Appendix D: Abstract Submitted for AAAR 2021 Conference | 42 |
| Appendix E: Abstracts Submitted for AAAR 2024 Conference | 43 |

LIST OF ILLUSTRATIONS

| <i>Number</i> | <i>Page</i> |
|---|-------------|
| 2.1 Schematic of the mask test apparatus showing the aerosol source, conditioning system, the chamber, the fixture apparatus for filter medium evaluation, and associated instruments and controls. | 7 |
| 2.2 Picture of the setup used for material (left) and mannequin (right) tests. | 8 |
| 3.1 Pressure drop versus flow rate for single masks. With labelling, N represents N95 respirators, K represents KN95 respirators, P represents procedural masks, and C represents cloth masks. | 12 |
| 3.2 Penetration for N1 with different flow rates. | 13 |
| 3.3 Penetration for K1 with different flow rates. | 14 |
| 3.4 Penetration for P1 with different flow rates. | 15 |
| 3.5 Penetration for C1 with different flow rates. | 16 |
| 4.1 Pressure drop of different mask combinations along with single mask data. | 19 |
| 4.2 Penetration of N2 with different masks worn on top of it. | 20 |
| 4.3 Penetration of K2 with different masks worn on top of it. | 21 |
| 4.4 Penetration of P2 with different masks worn on top of it. | 22 |
| 5.1 A drawing of the leaks on mask during inhalation (left). A circuit equivalent of our system (right). | 25 |
| 5.2 Sample graph of material and mannequin regression lines to show how the flow rate of leaks is found. | 26 |
| 5.3 Pressure drop values for material and mannequin tests for different masks: N1 (top left), K1 (top right), P1 (bottom left), C1 (bottom right) as a function of flow rate. | 27 |
| 5.4 Graph of flow rate vs leakage flow rate. | 28 |
| B.1 Linear plot of penetration of N2 with different masks worn on top of it. | 39 |
| B.2 Linear plot of penetration of K2 with different masks worn on top of it. | 40 |
| B.3 Linear plot of penetration of P2 with different masks worn on top of it. | 40 |

LIST OF TABLES

| <i>Number</i> | <i>Page</i> |
|---|-------------|
| 5.1 Resistance values without leaks (R_1) and with leaks (R_2). | 25 |
| A.1 Specification of masks. | 38 |

Chapter 1

INTRODUCTION

Throughout 2020, Severe Acute Respiratory Syndrome Coronavirus 2 (SARS-CoV-2), which causes the disease COVID-19, created an international crisis, both medically and economically. During COVID-19 pandemic, there have been 517 million reported cases and close to 6.3 million deaths from World Health Organization (WHO) as of May 13, 2022 (<https://covid19.who.int/>). Assuming a global population of 7.8 billion, this means that almost 7 in every 100 people have been infected with the virus. The massive spread of SARS-CoV-2 can be attributed to the three commonly accepted methods of virus transfer: contact, large droplet, and aerosol transmission (Morawska et al., 2020). Contact transmission is having direct contact with contaminated surfaces, which are known as fomites. Droplet transmission is for large droplets with a diameter greater than $5\ \mu\text{m}$ that fall close to where they were emitted. Xie et al. (2007) reported that these large droplets can get carried more than 6 m away when sneezing, more than 2 m away when coughing, and less than 1 m away when breathing. Aerosol transmission refers to small airborne particles with diameters less than $5\ \mu\text{m}$ that can travel for long distances and remain in the air for several hours.

There has been increasing evidence to support that aerosol transmission is a viable virus transmission pathway for COVID-19. At 65% relative humidity and 21-23°C, the half-life of SARS-CoV-2 is approximately 1.1 to 1.2 hours, which is similar to another coronavirus strain SARS-CoV-1 (van Doremalen et al., 2020). At $53\pm 11\%$ relative humidity and $23\pm 2^\circ\text{C}$, virus-containing aerosols were detected after 16 hours (Fears et al., 2020). Viable SARS-CoV-2 has been separated from air samples collected 2 to 4.8 m away from patients in their hospital rooms in the University of Florida Health Shands Hospital in Gainesville, Florida, USA (Lednicky et al., 2020). Furthermore, SARS-CoV-2 RNA was found in 4 of the 55 air samples taken less than 1 m from patients in hospitals in England (Moore et al., 2020). Ma et al. (2020) reported that 3.8% of air samples were positive for SARS-CoV-2 in a hospital located in Beijing, China, and an exhaled breath emission rate of $10^3 - 10^5$ RNA copies min^{-1} . In airborne infection isolation rooms at the National Centre for Infectious Diseases, Singapore, air samples from two out of three rooms tested positive for SARS-CoV-2, and the total virus concentrations in the air ranged from

$1.84 \times 10^3 - 3.38 \times 10^3$ RNA copies m^3 (Chia et al., 2020).

There have also been outbreak events that support the mechanism of aerosol transmission for COVID-19. There was an outbreak involving three families who sat at adjacent tables in a restaurant in Guangzhou, China (Li et al., 2020). One member in one of the families was infected with COVID-19 prior to going to the restaurant. It was later discovered that members of the two other families had become infected, yet no other patrons in the restaurant were infected. The three tables were in the path of an air-conditioning unit that confined the air, thus, the viral aerosols to this area. Because there was no physical human interaction (only some people sitting back-to-back) or fomite contact, aerosol transmission was likely the primary mechanism. There was a super spreading event that occurred when the Skagit Valley Chorale had a rehearsal on March 10, 2020, in Skagit Valley, Washington, USA. After the rehearsal, 53 out of 61 members of the chorale were confirmed to have contracted COVID-19 and two died. One person had cold-like symptoms prior to the rehearsal who later tested positive for COVID-19. The only plausible method for this to occur was aerosol transmission since physical interaction was minimal, reducing the possibility of contact transmission. The closest person to the original infected person was 1 m away during the rehearsal, reducing the possibility of droplet transmission (Miller et al., 2021).

Worldwide there are a number of different standards for testing and certifying masks and respirators. The test methods for measuring particle filtration efficiency in these standards vary in the type of aerosol used, the size distribution of aerosol, aerosol charge, flow rate through the respirator, and measurement system (Rengasamy et al., 2009). In the US, the National Institute for Occupational Safety and Health (NIOSH) and American Society for Testing and Material (ASTM) certify the masks and respirators based on the ability of filter media to prevent penetration of specific sizes and kinds of materials. NIOSH certifies respirators in one of nine classes based upon three levels of minimum filtering efficiency and resistance to filter degradation. These respirators are categorized into N, R, and P series respirators, depending on the type of aerosols used for testing. They further classified into types 95, 99, and 100 with minimum filtration efficiencies of 95%, 99%, and 99.97%, respectively. The NIOSH protocol for N-series respirators requires a polydisperse distribution of dried sodium chloride (NaCl) aerosol particles with count median diameter of $0.075 \pm 0.020 \mu\text{m}$ and a geometric standard deviation of < 1.86 . For R- and P-series respirators, NIOSH requires a polydisperse distribution of dioctyl phthalate

(DOP) particles with a count median diameter of $0.185 \pm 0.020 \mu\text{m}$ and a geometric standard deviation of < 1.60 . Similar to NIOSH, ASTM certifies the filtration of surgical masks into three levels based on testing for fluid resistance, breathability, bacterial filtration efficiency (BFE), particulate filtration efficiency (PFE), and flammability. For BFE and PFE certification, surgical masks are tested with $3.0 \pm 0.3 \mu\text{m}$ droplets containing *Staphylococcus aureus* and Polystyrene latex spheres of $0.1 \mu\text{m}$, respectively. Presently, due to the limited supply of NIOSH certified N95s, the U.S. Food and Drug Administration (FDA) allows the use of respirator certified under standards used in other countries such as FFP2 (Europe EN 149-2001), KN95 (China GB2626-2006), P2 (Australia, New Zealand AS/NZS 1716:2012) and DS/DL2 (Japan, JMHLW-2000), PFF2 (Brazil ABNT/NBR 13698:2011) and Korea first class (Korea KMOEL-2017-64) (<https://www.cdc.gov/niosh>).

To fully understand how masks perform on human faces, testing with mannequin heads is often used to evaluate the fit of masks. For a mannequin test done with SARS-CoV-2 virus, Ueki et al. (2020) found a reduction in the infective virus that passed through the mask (N95 respirators, cotton masks, procedure masks) compared to when the receiver was not wearing a mask. Bacteriophages and sodium chloride aerosol are commonly used to mimic viral aerosol inhalation. Bacteriophages have a similar size to viruses, but are not as dangerous. Sodium chloride matches the saline nature of respiratory particles that are emitted and inhaled. With sodium chloride aerosol, Pan et al. (2021) measured the filter efficiencies of procedure and cloth masks when inhaling and exhaling with two mannequins, varying which mannequin had a mask worn. Both masks had a better filtration efficiency for particles $> 1 \mu\text{m}$ than for smaller particles. Gao et al. (2016) found that increasing flow rate or humidity increased the penetration of sodium chloride particles while inhaling. The N95 respirator was fully sealed onto a mannequin inside of an exposure chamber with the aerosol generator, breathing simulator, aerosol size spectrometer and a condensation particle counter. Mannequin tests were carried out with various bacteriophages as well. With bacteriophage MS2 ranging in sizes 10-80 nm, (Bałazy, Toivola, Adhikari, et al., 2006) tested procedure masks and N95 respirators that were fully sealed onto a mannequin. For one of the N95 respirators tested, the penetration of particles was less than 5% at 30 and 85 LPM. One procedure mask tested had a peak penetration at 12% at 30 LPM, and 20.5% at 85 LPM. Wen et al. (2013) achieved above 95% in bacteriophage filtration efficiency for 7 procedure masks and 2 N95 respirators. For these experiments, the masks were sealed with silicon sealant onto the mannequin with an inhalation rate of 28.3 LPM.

Some studies have evaluated the performance of masks on human faces. Masks were tested on human faces (one man and one woman) with aerosol diameters from 0.02 to 3 μm at a temperature of 23-29.5°C. The filtration efficiencies of fitted masks were 97.9 \pm 0.5% for a new 3M 8120 N95, 38.1 \pm 11.4% for a procedure mask, 53.2 \pm 6.8% for Guangdong Fei Fan KN95, and 85.1 \pm 2.2% for Jia Hu Kang KN95 (Sickbert-Bennett et al., 2020). Mask efficiency levels of masks worn by one man was 26.5 \pm 10.5% for 3-layer woven cotton mask, 49.9 \pm 5.8% for a cotton bandana folded into a rectangle, 39.3 \pm 7.2% for single-layer woven polyester/nylon mask (Clapp et al., 2020).

The low efficiency measured when a mask is fitted onto a face or mannequin depends on both the filtration efficiency and leaks at the nasal and cheek area even when worn correctly. Leakage negates the benefits of a mask by allowing viral particles into the air due to exhalation. For 3M respirators with P100 filters tested on a mannequin, total inward leakage (TIL, during inhalation) increased with particle size and decreased with flow rate (more so from 30 LPM to 55 LPM than from 55 LPM to 85 LPM), but did not depend on breathing frequency in tests using combustion aerosols (He et al., 2014). In a study conducted with a mannequin with artificial leaks on the masks induced through needles, TIL increased with increasing leak size and flow rate. Higher efficiency N95 respirators and surgical masks showed lower TIL than lower efficiency ones, suggesting that the mask filtration efficiency plays a role in leakage (Rengasamy et al., 2014). In a study comparing mannequin tests of filtration efficiency with the ones beforehand using human subjects, it was found that the penetration through the leakage was much higher than through the masks tested (N95 respirators and surgical masks). For N95 respirators, the penetration through leaks was, on average, an order of magnitude greater than through the masks, and significantly increased with particle size (Grinshpun et al., 2009). These studies all support the hypothesis that leakage is a significant pathway by which particles escape instead of being filtered through the masks. Hence, it is important to understand the characteristics of these leaks.

Double masking is has been recommended as a way to increase protection, but few scientific studies have been conducted to evaluate the performance. When people do not have access to N95 or KN95 respirators (generally better-performing masks), they may resort to wearing a cloth mask and procedure mask together in order to increase mask performance that could hinder breathing for some wearers. Masks should be worn even as more people are being vaccinated to prevent the

spread of another potential variant of COVID-19. The cost of wearing a quality mask every day is a high premium for front-line and essential workers. The Centers for Disease Control and Protection (CDC) has recommended wearing two masks or using a mask brace and other means to improve fit in order to improve protection of the face covering (<https://www.cdc.gov/coronavirus/2019-ncov/your-health/effective-masks.html>). The low costs of cloth and procedure masks make this method attractive, so it is important to understand the performance of wearing two masks. In order to maximize protection and, potentially, to attain an efficiency of greater than 90% for 1 μm or larger, it has been suggested that a cloth mask be worn on top of a procedure mask or three-layer mask with the outer layers being a flexible, tightly woven fabric and a middle layer with a non-woven high-efficiency filter material (Gandhi & Marr, 2021). In a study by the CDC conducted with mannequin heads using 0.1-7 μm KCl particles, when the source mannequin was not masked or double masked (cloth mask covered on top of procedure mask) and the receiver was wearing double masks, the cumulative exposure of the receiver was reduced by 83% and 96.4% respectively (Brooks et al., 2021). When the source was not masked, or the source had an unknotted procedure mask, and the receiver was wearing an unknotted procedure mask, the cumulative exposure of the receiver was reduced by 7.5% and 84.3% respectively, supporting the hypothesis that wearing double masks is better than using a single procedure mask.

The goal of this study is to evaluate different types of masks as well as various combinations of masks. There is not much literature about measuring the performance of double masks, even though it has been recommended by public health agencies. Penetration and pressure drop will be the major metrics used to evaluate mask performance. Penetration is how many particles get through the mask. The pressure drop affects the comfort of the mask wearer, but the pressure drop that affect comfort varies from person to person. In this study, mannequin testing provides insights into how mask performance differs on a human face from that measured in a perfectly sealed test. The two tests will also be compared to give an understanding of leakage.

*Chapter 2***MATERIALS AND METHODS****2.1 Masks**

The masks were chosen based on the results from a recent paper by our lab. The types of masks that were tested were N95 respirators, KN95 respirators, procedure masks, and cloth masks. The specifications of the masks selected are shown in Table A.1. Four different masks from each category were evaluated in order to be able to notice some variance between masks of the same type, but only results from two sets of masks will be reported for conciseness. During all the tests, the masks were intact to emulate the real world usage of masks compared to studies done with filter holders, which allow for the filtration area to be known accurately.

2.2 Experimental Setup and Procedure

The experimental set-up used to assess the performance of masks is shown in Figure 2.1. The effectiveness of the masks for inhalation was evaluated. Polydisperse aerosol was generated by atomizing a dilute solution (1% w/v) of NaCl with an in-house constant flow rate nebulizer. The aerosol humidity and charge state were conditioned by passing the flow through a Nafion membrane diffusion drier and a Soft X-Ray source, respectively. The aerosol flow was diluted with particle-free air to adjust particle concentration at desired levels, and was introduced into a 21 L stainless steel chamber. To seal the mask fully to a substrate for measurements of the filtration efficiency of the mask material, a rubber gasket was placed on the bottom, then the mask sample, and on top of that, a wooden piece with a circular hole and clamped down with four C-clamps. The masks were kept intact for these material tests, which only consider the effects of the mask material and minimize leaks. The setup for the material tests is shown in Figure 2.2 (left). For the double mask tests, the layering scheme was repeated with one mask on top of another. Sampling ports on the substrate of the chamber allowed probing of the aerosol concentration and flow pressure independently, both upstream and downstream of the mask sample. The performance of mask samples was characterized with a Scanning Electrical Mobility Spectrometer system, consisting of a Kr⁸⁵ charge conditioner, a TSI 3081 Long-column Differential Mobility Analyzer (LDMA) and a “MAGIC” model 200/210 water-based Condensation Particle Counter (CPC) from Aerosol

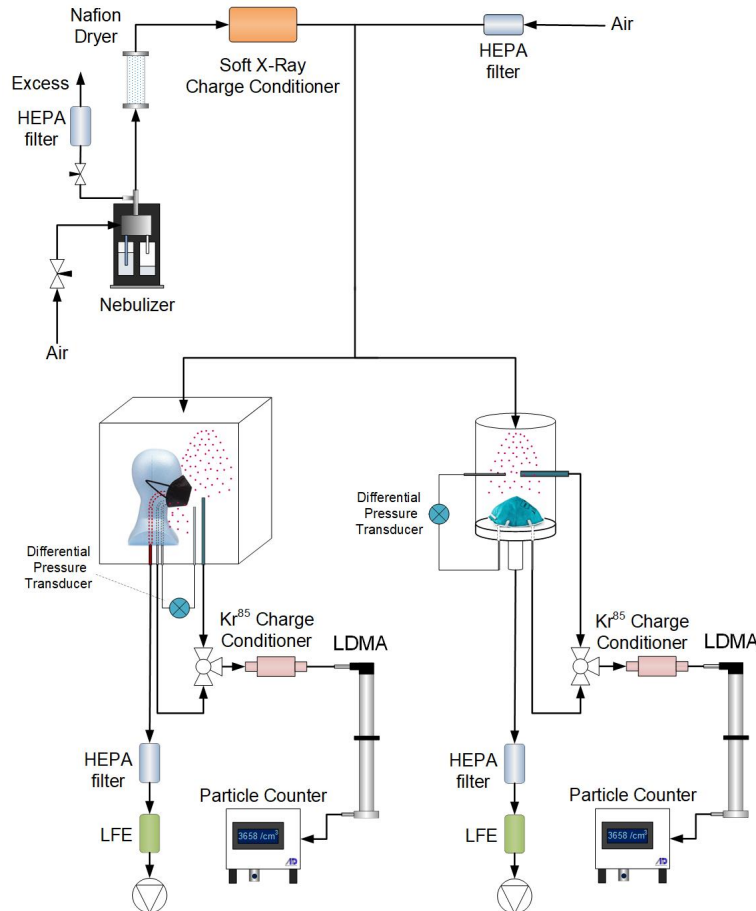


Figure 2.1: Schematic of the mask test apparatus showing the aerosol source, conditioning system, the chamber, the fixture apparatus for filter medium evaluation, and associated instruments and controls.

Dynamics Inc (Hering et al., 2014, 2019). The LDMA was calibrated with PSL nanoparticles at a size of 150 nm to ensure that the system was accurately yielding counts in a Gaussian shape that has a center of around 150 nm. Before any masks were tested, the noise of the system for particle concentration and pressure drop was checked; it was found to be minimal. The LDMA was used at 2.8 LPM sheath and 0.3 L/min aerosol flows, and provided particle size distribution measurements in the 30-800 nm range. The scan time for this system was 4.5 minutes. A 3-way valve was employed to switch the sample lines in order to probe the aerosol upstream and downstream of the masks. Sampling tubes were kept as short as possible to minimize particle losses. The pressure drop through the masks was measured with a Dwyer Model 607-4 differential pressure transducer. To vary the flow rate simulated when inhaling, a GAST G608EX vacuum pump was used to draw the desired total flow rate through the mask.

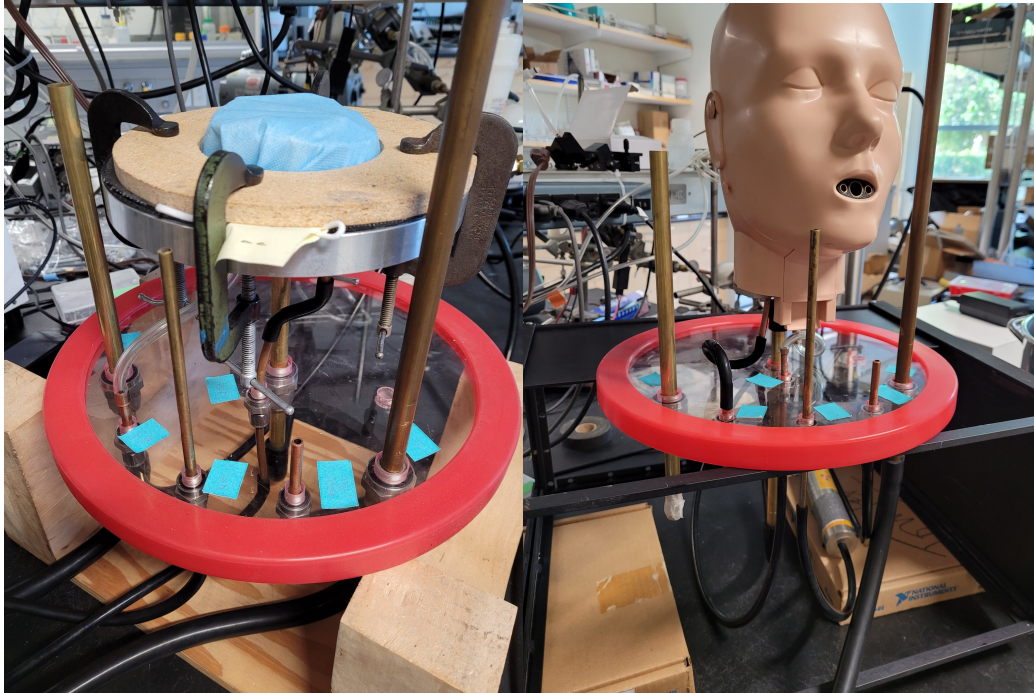


Figure 2.2: Picture of the setup used for material (left) and mannequin (right) tests.

The mannequin setup is shown in Figure 2.2 (right). The mannequin head used in these experiments was the Prestan Ultralite Mannequin. The inside of the mannequin was fitted with piping that connects the mouth (input) and the bottom of the neck (output). The mouth of mannequin is where the particles will enter into our testing system after penetrating a mask attached via ear loops without additional sealing. The tubing at the bottom of the neck will be directed to our measurement instruments. There are three different pipes within the mannequin. The first one in the center that is slightly larger than the other two is where the vacuum pump is connected to simulate different flow rates. The pipe to the right is connected to the CPC, which generates particle counts. The pipe to the left is connected to the pressure transducer. The bottom platform is the same as the one used for the material tests. The top parts of the setup, the platform with C-clamps and the mannequin head, can be interchanged, but the tests were done through separate time periods; repeated switching the top parts of the setup was avoided for consistency in tubing. For the pressure drop data from the mannequin, our experiments utilized a "Fix the Mask" band to seal the KN95 respirator, procedure mask, and cloth mask to the mannequin head in order to ensure a tight seal to the face and to enable a direct measurement of the pressure drop through the mask or mask combination. No additional tightening mechanisms were used for the N95 respirator. The fit on the mannequin was not as

effective as the nearly complete seal achieved in the material tests.

2.3 Mask performance metrics

Particle penetration: The performance of masks was assessed by calculating the fraction of particles penetrating through the mask. The flow rates tested were 5, 30, and 85 LPM for material tests, and only 30 LPM for mannequin tests. 5 LPM represents a resting breathing rate. 30 LPM corresponds to a breathing rate while performing light exercise, while 85 LPM corresponds to a breathing rate while conducting heavy exercise (Bałazy, Toivola, Reponen, et al., 2006). The penetration was calculated using Equation 2.1:

$$penetration = \frac{N_{down}}{N_{up}} \quad (2.1)$$

where N_{down} and N_{up} is the downstream (inside the mask) and upstream (outside the mask) particle number concentration, respectively.

Pressure drop: The pressure drop was measured with a differential pressure transducer that probed the pressure difference between points outside of the mask and inside the mask. Equation 2.2 shows the calculation used to find the pressure drop. Pressure drop was evaluated for 7 different flow rates (5, 20, 30, 50, 60, 70, 85 L/min). For the material tests, the correlation of pressure drop with flow rate should be linear. For the mannequin, since the fit was imperfect, the correlation of pressure drop with flow rate should be linear but not fit as well compared to the material test.

$$\Delta P = P_{up} - P_{down} \quad (2.2)$$

where P_{down} and P_{up} is the downstream and upstream pressures, respectively.

2.4 Data Analysis

To analyze the data acquired, MATLAB was used to generate all the plots for pressure drop and penetration. For pressure drop plots, the pressure drop values over the size range were averaged and plotted as points for each flow rate. A linear regression was fitted to the data of flow rate versus pressure drop in order to generate the dotted line shown on the graphs. For the penetration plots, three scans were conducted for both the upstream and downstream particle counts. For the upstream and downstream particle counts, the average of the three scans was used and fitted to a best fit curve. Then, the penetration as a function of particle size was calculated as the ratio of the fitted concentration versus size curve obtained downstream of the

mask to that obtained upstream. The resulting penetration plots are reported as fit curves. This use of fitted curves yields more consistent penetration estimates than would be obtained by taking the ratio of individual measurements from noisy data. The uncertainty of the particular penetration was estimated with a propagation of errors analysis. This analysis of fitting lines for the penetration graphs and utilization the measure of propagation of errors were done by a postdoc in Richard Flagan's lab, Buddhi Pushpawela, but I wanted to provide a brief summary of how these penetration plots made.

Chapter 3

SINGLE MASK RESULTS

3.1 Pressure Drop

The results from the pressure drop material tests are shown in Figure 3.1. In the figure, N represents N95 respirators, K represents KN95 respirators, P represents procedural masks, and C represents cloth masks. The tested K95 respirator have the highest pressure drops and procedure masks have the lowest pressure drops among all masks for all the flow rates examined. The pressure drop increased linearly with flow rate with $r^2 > 0.98$. The pressure drops through the N95 respirators and cloth masks are close in value, which can be analyzed with an empirical equation was developed by C.N. Davies in 1973 to find pressure drop for fibrous media as shown below in Equation 3.1 (Huang et al., 2013).

$$\Delta p = \frac{\eta \chi V 64 \alpha^{1.5} (1 + 56 \alpha^3)}{d_f^2} \quad (3.1)$$

where η is the gas viscosity, χ is the filter thickness, V is the face velocity, α is the packing density, and d_f is the fiber diameter. For our experiment, the gas viscosity is constant since the same NaCl aerosol is being utilized while the face velocity is associated with the flow rate. The flow rate is the face velocity multiplied by the thickness of the mask. According measurements made using a caliper, the thickness of the N95 respirator and cloth mask tested both were around 1.5 mm. Since the thicknesses of the masks are nearly the same, then the face velocity must also be the same since the flow rate used were the same for both masks. This study did not investigate the detailed physical structure of the fabrics (i.e., the packing density and fiber diameter). Assuming similar values of packing density and fiber diameter for both masks, the similarity in pressure drops of N95 respirator and cloth mask could be attributed to the similar thickness of the two masks with the data found in this study.

The N95 respirator has a pressure drop of 64 Pa at 85 LPM. According to the Code of Federal Regulations Title 42 Part 84.172, the maximum inhalation pressure drop for N95 grade respirators is 343 Pa at 85 LPM, so our N95 respirator is well below the maximum value (Rengasamy et al., 2009). At 85 LPM with NaCl aerosol sized 20-500 nm, Eninger et al. (2008) reported pressure drops ranging from 67-82 Pa

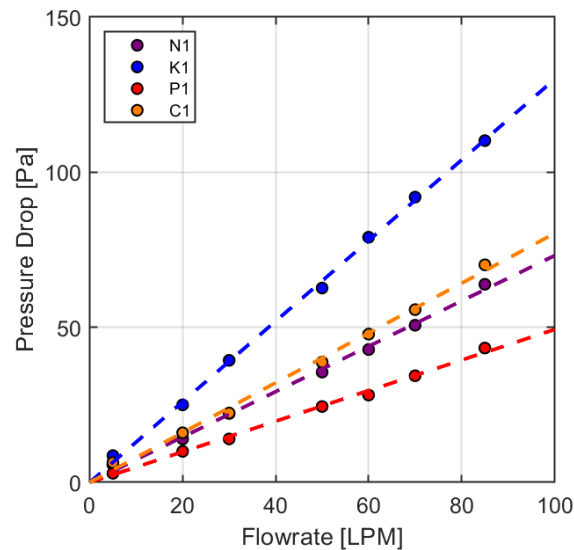


Figure 3.1: Pressure drop versus flow rate for single masks. With labelling, N represents N95 respirators, K represents KN95 respirators, P represents procedural masks, and C represents cloth masks.

for similar N95 respirators, slightly higher than our value. Several studies reported a range of pressure drops for N95 respirators at 85 LPM that included our value: 83 ± 25.7 Pa (Jung et al., 2014) and 67.3 ± 8.8 Pa (Cho et al., 2011). In another study in which masks were fully sealed, one N95 respirator labeled NIOSH-FFR 2 tested had pressure drop of 61 Pa (extremely close to our value of 64 Pa) at 85 LPM (Brochot et al., 2020). Eninger et al. (2008) and Jung et al. (2014) reported the pressure drops slightly higher than our value at 30 LPM.

The KN95 respirator has a pressure drop of 110 Pa at 85 LPM. According to Chinese legislation GB2626-2019, the maximum inhalation pressure drop for KN95 grade respirators is 210 Pa at 85 LPM and our KN95 respirator is lower than this maximum value (Brochot et al., 2020). In a different study, a KN95 respirator labeled KN95-FFR 1 was at 100 Pa (close to our value of 110 Pa) (Brochot et al., 2020). At 30 LPM, the procedure mask tested attained a pressure drop of 14 Pa and was within the range of values found previously: 11.8-17.7 Pa (Guha et al., 2015) and 10-18 Pa (Weber et al., 1993). At 5 LPM, the pressure drop for procedure masks ranged from 1.96-2.94 Pa, which includes our value of 2.9 Pa (Guha et al., 2015). The mean pressure drop of cloth masks is 19.93 Pa at 30 LPM similar to our value of 22 Pa, and 66.5 Pa at 85 LPM, similar to our value of 70 Pa (Jung et al., 2014).

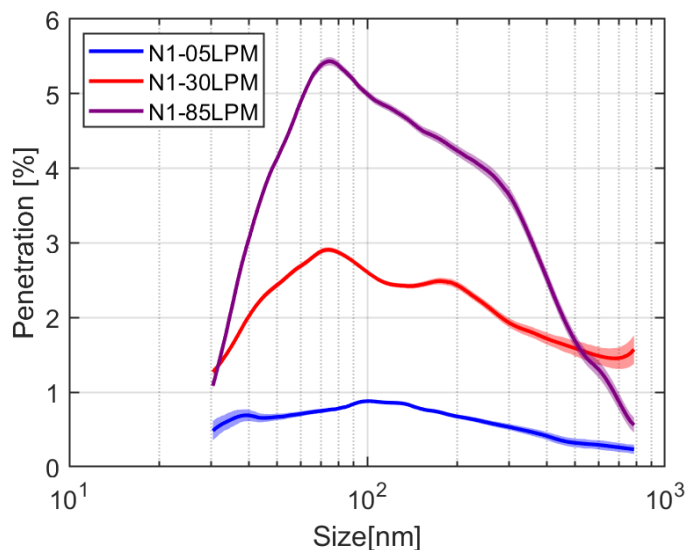


Figure 3.2: Penetration for N1 with different flow rates.

3.2 Penetration

The penetration was calculated for three different flow rates of 5, 30, and 85 LPM. 5 LPM represents a resting breathing rate. 30 LPM corresponds to a breathing rate during light exercise. 85 LPM corresponds to a breathing rate during heavy exercise. The results for penetration with varying flow rates for an N95 respirator is shown in Figure 3.2. The highest penetration value along with most penetrating particle size (MPPS) for N1 for all flow rates: 0.88% at 102 nm for 5 LPM, 2.91% at 76 nm for 30 LPM, 5.44% at 75 nm for 85 LPM. For the N95 respirator, the penetration increased with flow rate, and decreased slightly in MPPS when the flow rate increased from 5 to 30 LPM and remained constant in MPPS when the flow rate increased from 30 to 85 LPM.

Our MPPS values for 85 LPM will be compared with values found in other studies. The highest penetration value and MPPS were lower than what was observed in this study: nearly 2% at around 25 nm (Brochot et al., 2020), 4.8% at 45 nm (Eninger et al., 2008), and 4% at around 45 nm (Hao et al., 2021). Some studies had a similar highest penetration value with 5.8% at around 50 nm (Huang et al., 2007) and 6% at 45 nm (Bałazy, Toivola, Reponen, et al., 2006). However, all of the studies had lower MPPS than our study. A potential reason is that this N95 respirator was tested multiple times, which may have depleted stored charge in the filter and reduced the strength of the electret effect. The range of our penetration data over this size range of 0.5-5.5% is similar to that reported in other studies (Bałazy, Toivola, Reponen,

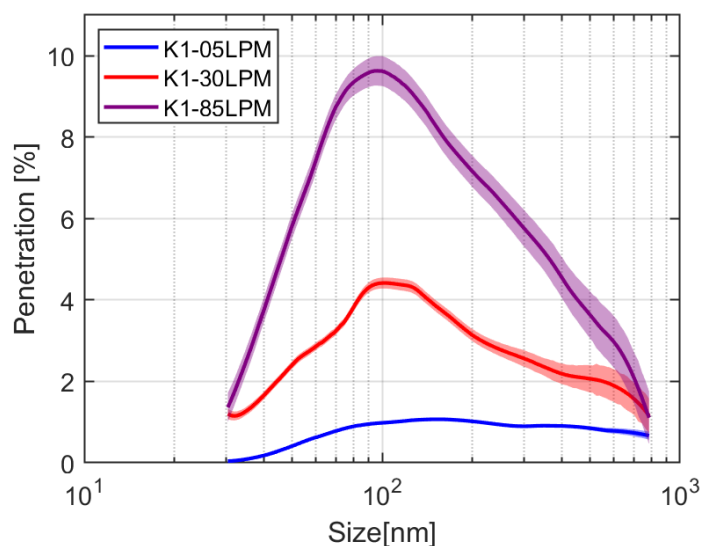


Figure 3.3: Penetration for K1 with different flow rates.

et al., 2006; Eninger et al., 2008). In our data, particles of sizes of 50-100 nm have penetration greater 5% at 85 LPM, which occurs at sizes 33-73 nm in (Bałazy, Toivola, Reponen, et al., 2006). N95 respirators are certified to remove at least 95% of particles for sizes greater than 300 nm, but for some portions of the SARS-CoV-2 virion diameter range of 80-120 nm, more than 5% of particles are penetrated, which can expose people to deadly virus when they expect their masks to block most particles over the entire size range (Liu et al., 2020).

For 30 LPM, the highest penetration value and MPPS were lower than what was observed in this study: 2.8% at 50 nm (Bałazy, Toivola, Reponen, et al., 2006) and 1.4% at around 45 nm (Eninger et al., 2008). The range of our penetration data over this size range at 30 LPM of 1-3% is the same as what is found by other studies (Bałazy, Toivola, Reponen, et al., 2006; Eninger et al., 2008). For aerosols with sizes less than 300 nm at 5 LPM, a N95 respirator had a size-averaged penetration of 0.3% at 5 LPM, which is less than than our estimated value of around 0.5% (Sheets et al., 2020).

The results for penetration with varying flow rates for a KN95 respirator is shown in Figure 3.3. The highest penetration value along with the size at which highest penetration occurs for K1 for all flow rates: 1.07% at 154 nm for 5 LPM, 4.42% at 102 nm for 30 LPM, 9.63% at 96 nm for 85 LPM. For the KN95 respirator, the penetration increased with flow rate, and decreased slightly in MPPS when the flow rate increased from 5 to 30 LPM and slightly shifted in MPPS when the flow rate

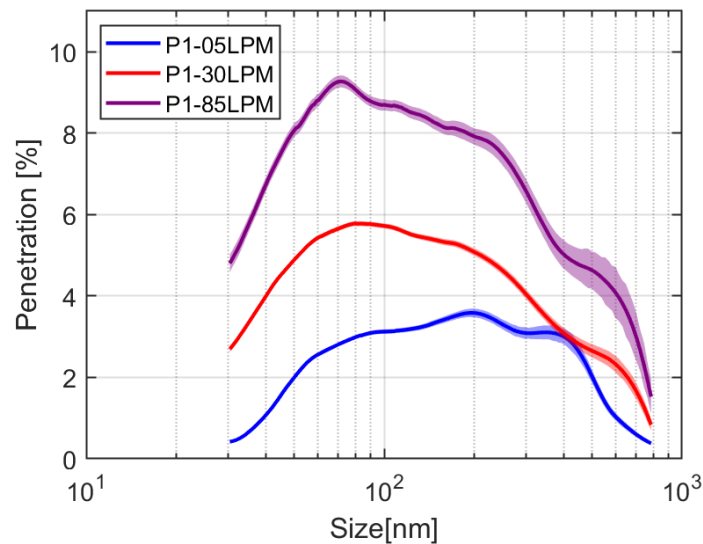


Figure 3.4: Penetration for P1 with different flow rates.

increased from 30 to 85 LPM. At 85 LPM with NaCl particles sized 20-600 nm, a KN95 respirator with label K95-FFR 2 had most penetrating particle size at around 40 nm with penetration varying from 3-7%, which are both lower than observed in our study (Brochot et al., 2020). At 30 LPM, a study found penetration was around 0-2% for 300 nm and 0-1% for 500 nm, both of which are lower than our values for those sizes (van der Vossen et al., 2021). For aerosols with sizes less than 300 nm, a KN95 respirator labeled KN95#1 had a size-averaged penetration of 1% at 5 LPM, which is greater than what our data would yield of around 0.5% (Sheets et al., 2020).

Figure 3.4 shows the results for penetration with varying flow rates for a procedure mask. The highest penetration value along with the size at which highest penetration occurs for P1 for all flow rates: 3.58% at 194 nm for 5 LPM, 5.78% at 80 nm for 30 LPM, 9.27% at 71 nm for 85 LPM. The procedure mask decreased significantly in MPPS when the flow rate increased from 5 to 30 LPM and decreased slightly in MPPS when the flow rate increased from 30 to 85 LPM. In a study with NaCl aerosol using flow rate of 3 LPM, a procedure mask had 95% filtration efficiency or better (corresponding to 5% penetration or less) for sizes from 20 to 750 nm (Crilley et al., 2021). For particles smaller than 100 nm, the average filtration efficiency ranged from 95.5-98.5% (penetration of 1.5-4.5%), which is include the value of around 2% that our data would yield. In a study with MS2 virus aerosol sized 10-80 nm, surgical masks labeled SM2 had a peak penetration of around 13% at 65 nm

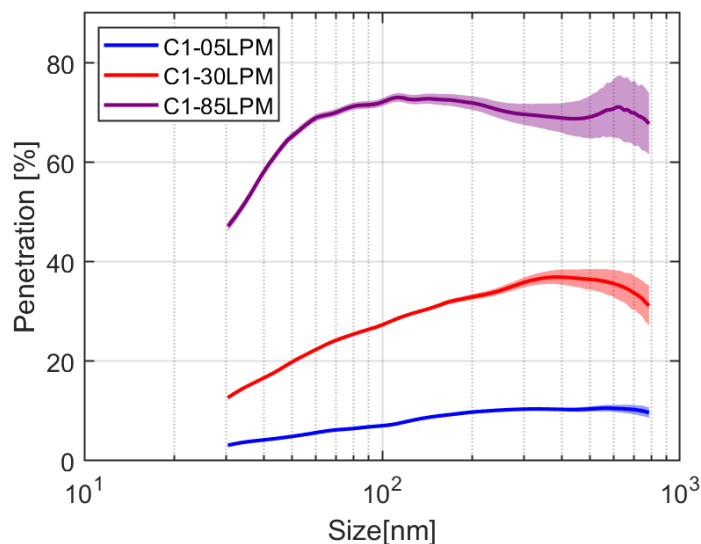


Figure 3.5: Penetration for C1 with different flow rates.

at 30 LPM, which is twice the percentage we obtained (Bałazy, Toivola, Adhikari, et al., 2006). At 85 LPM, the maximum penetration is 20% at 60 nm, which is the same size but the penetration value is doubled. The range of the penetration is much greater than what we see. The fact that the experiments were conducted with MS2 virus may have affected the penetration.

Figure 3.5 shows the results for penetration with varying flow rates for a cloth mask. The highest penetration value along with the size at which highest penetration occurs for C1 for all flow rates: 10.58% at 567 nm for 5 LPM, 36.93% at 385 nm for 30 LPM, 73.04% at 114 nm for 85 LPM. For 5 and 30 LPM, the penetration is mostly increasing with size, which is different than the Gaussian shaped penetration curve that were observed in all of the other masks and for C1 at 85 LPM. The cloth mask decreased in MPPS as flow rate increased. There is a lot of literature comparing different fabrics such as silk, cloth, and flannel, but not many that investigate cloth masks with similar conditions set forth in this study.

Comparing all of the masks, the peak penetration is lowest for N95 respirators at all flow rates, and the peak penetration is highest for cloth masks at all flow rates. At 5 LPM, KN95 and N95 respirators have a similar penetration range of 0-1% with the KN95 having a slightly greater peak penetration than the N95. The penetration curves for KN95 and procedure masks are similar in range at 85 LPM. The peak penetration is lower for KN95 respirators than that of procedure masks at 5 and 30 LPM. The respirators and the tested procedure mask have lower peak penetration

than the cloth mask because these masks utilize electrostatic interaction to filter particles in addition to impaction, interception, and Brownian motion. The cloth mask is a mechanical mask, which utilizes impaction, interception, and Brownian motion to capture particles. For all masks, the peak penetration increases with flow rate in agreement with other papers (Bałazy, Toivola, Reponen, et al., 2006; Eninger et al., 2008; Huang et al., 2013). The reason this occurs is that the higher flow rate provides a higher chance for all particles to penetrate through the mask.

In terms of MPPS considering all masks, the cloth mask had the highest MPPS values for all flow rates. The N95 respirator had the lowest MPPS at 5 and 30 LPM, yet the procedure mask had the lowest MPPS at 85 LPM (N95 respirator has a MPPS value that was 4 nm higher than the procedure mask). This displays that the N95 respirator dramatically reduces the MPPS across all flow rates due to the strong electret effect. There have been studies that support that electret masks tend to have lower MPPS than mechanical masks (cloth mask) (Bałazy, Toivola, Reponen, et al., 2006; Huang et al., 2013). There was a significant shift observed in MPPS for the cloth mask with increasing flow rate; however, the procedure mask, N95 respirator, and KN95 respirator had a similar MPPS from 5 to 30 LPM and a slight shift from 30 to 85 LPM. Hence, for cloth mask with increased flow rates, the effectiveness of diffusion and electrostatic attraction (mainly affecting small particles) decreases, while that of impaction (mainly affecting large particles) increases. In these experiments, the tested cloth mask was the only mask with a mechanical filter. Some procedure masks are also mechanical, but it depends on the brand and materials utilized. In a study, a theoretical comparison between mechanical and electret masks was conducted. The mechanical mask with no charge density yielded decreasing MPPS with increasing face velocity (Huang et al., 2013). The electret mask with charge density has a significant decrease in MPPS from 0.5 to 1 cm s^{-1} and slight decrease in MPPS from 1 to 3 cm s^{-1} . The observations made for mechanical and electret masks matches our results for all masks.

Chapter 4

DOUBLE MASK RESULTS

This experimental work is published in *Aerosol Science and Technology* as "Is Double Masking Even Worthwhile?" (Chea et al., 2024).

4.1 Experimental Reasoning

To start off the discussion of the effectiveness of double masking, the results from a different set of masks was utilized than that discussed in the section about single masks. The reason is that the data for the double mask combinations fit more with the initial interpretation of what would happen as well as some of the plots from the other set had some phenomenon that we could not explain. Hence, I will not repeat the analysis of the single masks pressure drops and penetration; however, the data for single masks will appear as a reference to understand the trends seen when double masking. All penetration tests done for double masks were conducted at a flow rate of 30 LPM.

There are a total of seven combinations tested for pressure drop and a total of six combinations tested for penetration (KN95 and N95 combination was not tested). All single mask types were tested with a procedure and cloth mask on top of them since these two masks are more cost-effective compared to KN95 and N95 respirators. Usually, double mask combinations are worn to maintain the quality of the bottom mask and allow the bottom mask to be worn multiple times. However, two identical mask types worn on top of each other were not tested since the behavior should reflect the single mask. We tested a procedure mask on top of a cloth mask and also a cloth mask on top of a procedure mask in order to check if the results were consistent and since these two mask combinations can be worn interchangeably since cloth and procedure masks are similar in cost-effectiveness. The combination of KN95 and N95 respirators were tested for the purposes of consistency, but this combination is not very commonly utilized among the public.

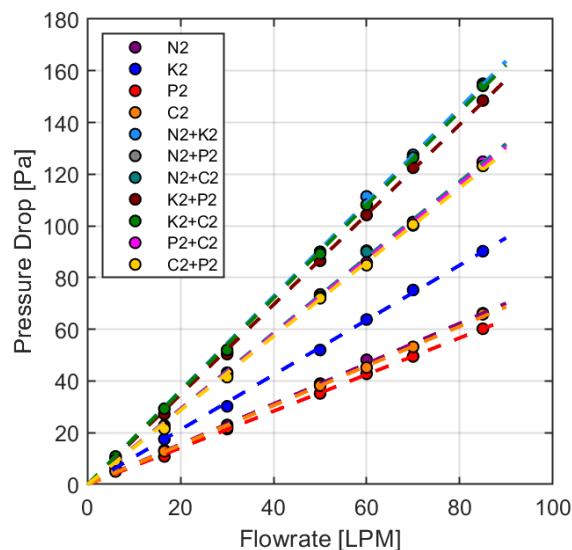


Figure 4.1: Pressure drop of different mask combinations along with single mask data.

4.2 Pressure Drop

The results of pressure drop values from single and double masking are seen in Figure 4.1. In the legend, the label "N2+K2" would mean that the KN95 was worn on the top of the N95 respirator with the bottom mask listed first then the top mask listed second. These results are from the material tests where leaks would not occur. All the pressure drops were increasing linearly with flow rate with a $r^2 > 0.98$. Out of all combinations, the N95 and KN95 combination had the highest pressure drop since both individual masks have higher pressure drops than cloth and procedure masks. The combinations with the lowest pressure drop are both variations of cloth and procedure masks. Another trend is that all combinations involving KN95 respirators have higher pressure drop values than all other combinations because the KN95 respirator has the highest single mask pressure drop. An important observation is that the sum of the pressure drop of the individual mask is similar to when two masks are worn together. For example, at 60 LPM, a single KN95 respirator has a pressure drop of 68.5 Pa, and a single procedure mask is at 40.3, and for K2+P2, the pressure drop observed around 108 Pa, which is very close to the sum of the pressure drops found for the individual masks. This phenomenon is what we expect when two masks are layered since air flow has to go through both masks and hence the pressure drop would be additive, assuming that the setup used ensured no leaks. Because of this higher pressure drop seen for two masks compared to a single mask, there is some reduction in breathability when wearing double masks.

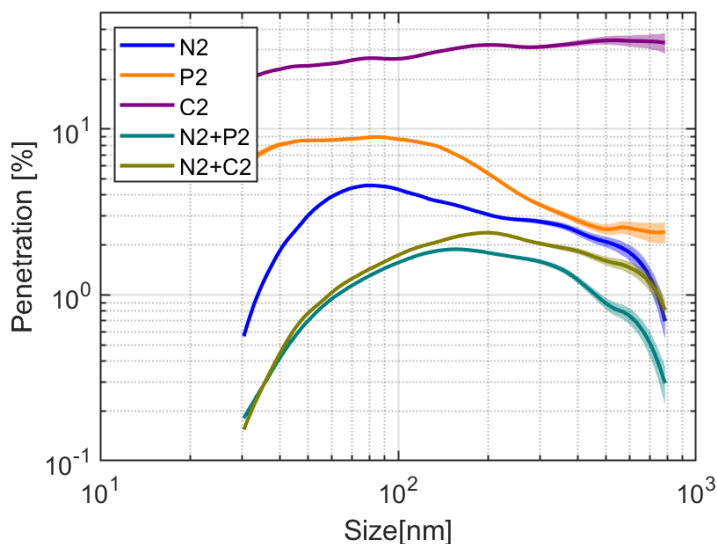


Figure 4.2: Penetration of N2 with different masks worn on top of it.

4.3 Penetration

Figure 4.2 shows the penetration of combinations involving an N95 respirator along with the individual masks. The penetration curves of both combinations are similar, from 30 to about 90 nm. Yet, the penetration of N2+P2 is lower than N2+C2 over most of the size range except when particle size is less than 35 nm. This exception occurs because there are a low number of counts at very small sizes or possibly some errors at the tails associated with fitting data with a moving average on Matlab. When considering the penetration over two masks, the simple trend should be that the penetration values should be multiplicative since the particles that pass the first mask are the only ones that have a chance to pass through the second mask, unlike the single mask case where penetration is solely considering the ambient particle counts. Hence, N2+P2 should have a lower penetration than N2+C2 since the penetration through P2 is lower than C2. When the penetration curves are multiplied together, the mask with the lower penetration values should yield a lower penetration in the double mask scenario. As the size increases from 80 nm to around 200 nm, the difference in penetration between the two combinations generally increases as well and can be seen more clearly with a linear plot in Figure B.1. This occurs because the penetration values of the procedure mask suddenly decrease starting from 80 nm onwards at a rate greater than the N95 in comparison to the cloth mask, which has penetration increasing over the size range. The decrease in penetration for procedure masks will cause the penetration of the combination N2+P2 to be lower than N2+C2. This observation validates the multiplicative nature

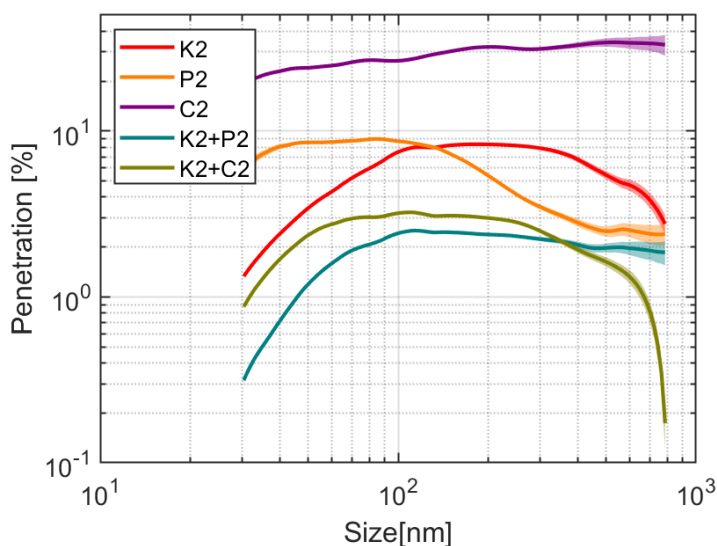


Figure 4.3: Penetration of K2 with different masks worn on top of it.

of penetration of masks when applied to double masking.

The peak penetration value along with the size at which peak penetration occurs: 4.6% at 80 nm for N2, 9% at 84 nm for P2, 34.3% at 538 nm for C2, 1.9% at 157 nm for N2+P2, and 2.4% at 198 nm for N2+C2. An observation is that the most penetrating particle size shifts from under 100 nm for an N95 respirator to greater than over 100 nm for the double mask combinations. There have been studies that support that electret masks tend to have lower MPPS than mechanical masks (cloth mask) (Bałazy, Toivola, Reponen, et al., 2006; Huang et al., 2013). Some procedure masks can be electret, but most of which the public purchases are not. When used in combination with a mechanical mask, the N95 respirator combination loses its electret features. The reason that this occurs is with the procedure or cloth mask serving as the top layer of the combination with higher MPPS, there are more larger particles that penetrate through mechanical masks, which can potentially penetrate through the electret N95 respirator. There are proportionally more large particles outside the mask in the double mask case than in the single N95 respirator case. Even though the N95 respirator has low penetration values for larger sizes, the existence of more large particles due to lack of filtration by mechanical masks yield a larger MPPS for the combinations than a usual N95 respirator.

Figure 4.3 shows the penetration of combinations involving a KN95 respirator along with the individual masks. The peak penetration value along with the size at which peak penetration occurs: 8.3% at 186 nm for K2, 2.5% at 114 nm for K2+P2,

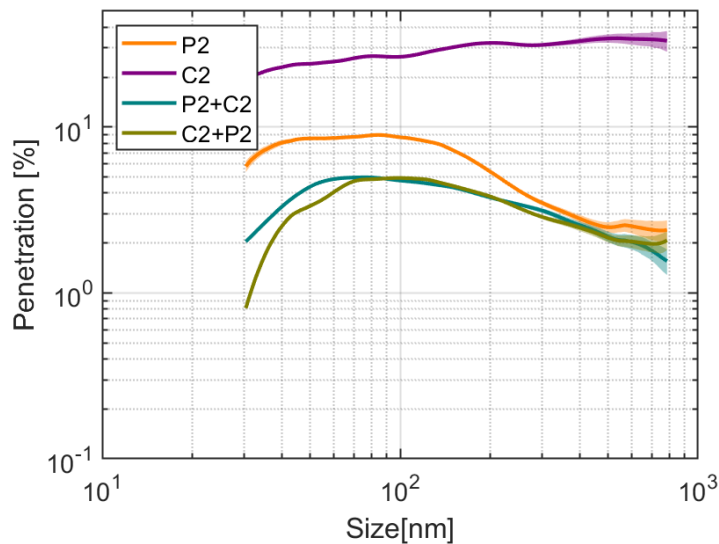


Figure 4.4: Penetration of P2 with different masks worn on top of it.

and 3.2% at 110 nm for K2+C2. K2+P2 has lower penetration percentages from 30-350 nm, yet K2+C2 has lower penetration from 350-800 nm. The MPPS of both combinations involving K2 are similar to the secondary local maximum in the K2 penetration curve that occurs at around 130 nm. For K2+P2, P2 has higher penetration than K2 until around 140 nm, so when particles penetrate past the first layer of P2, the highest penetrating size from 30-140 nm for K2 is around that secondary local maximum of 130 nm. The shape of K2+C2 seems to resemble the shape of the K2 penetration curve, a concave down pattern with a maximum between 100-200 nm. This similarity appears because the penetration curve of the cloth mask is linear increasing, which is similar to the distribution of particles introduced to a single K2 mask for the lower half of the size range. However, there are some differences in both penetration curves because the particles that the single mask are exposed resemble a Gaussian curve. For the upper half of the range, the number of particles provided to the single mask decrease from the maximum instead of increase, as seen with the cloth mask penetration curve. The K2+P2 curve is almost slightly increasing, starting from the MPPS of 120 nm. Based on the multiplicity of penetration of two masks, the penetration values of K2+P2 should always be lower than K2+C2 since penetration values of P2 are even lower than K2 starting from 120 nm. The reason this deviation from the ideal multiplicity of penetration could be due to different deposition mechanisms and fiber sizes.

Figure 4.4 shows the penetration of both possible combinations of cloth and procedure masks. The peak penetration value along with the size at which peak penetration occurs: 9% at 84 nm for P2, 34.3% at 538 nm for C2, 5% at 78 nm for P2+C2, and 4.9% at 98 nm for C2+P2. Overall, either combination of cloth and surgical masks yield a similar shape in the penetration curve over size, which is almost similar to the shape of the penetration curve of P2. Based on the multiplicative nature of two mask penetration, it is expected that the penetration curves for both combinations should be almost identical. However, through this test, the particles that penetrate the first mask do play a role in deviating the penetration curves slightly because the particles that the second mask on the bottom is exposed it is completely determined by how well particles penetrate through the first mask on top. The major difference is that C2+P2 has lower penetration than P2+C2 from 30-90 nm. This may occur because the penetration curve of P2 is increasing steadily from 30-90 nm and with P2 on top of C2, there is the effect of a lower amount of particles in that size range having the chance to pass through C2 after P2. With our setup, the DMA delivers more particles of smaller size and fewer particles of larger sizes, so this lower penetration of P2 in a smaller size range could affect the penetration values immensely. In contrast, with C2 on the top of P2, many more particles with an almost linear penetration distribution for C2 pass through, allowing for a higher penetration over both masks as a combination.

Comparing all combinations, the combination of N2+P2 has the lowest peak penetration value at around 2%. The combinations with KN95 respirators had the peak penetration value in the middle between combinations with N95, and P2 and C2. Either combination of P2 and C2 has the highest peak penetration percentage at around 5%. This order of peak penetration values makes sense because N95 respirators have the lowest peak penetration value out of all of the masks, while the cloth mask has the highest peak penetration. In terms of the MPPS, the combinations with N2 had that the highest values for MPPS at around 200 nm. The combinations of cloth and procedure masks had the lowest MPPS. In addition, some of the penetration curves for the combinations matched one of the curves for a single mask involved in the combination. Both combinations of C2 and P2 resembled the curve for only P2. The curves for the combinations with K2 matched the curve for K2, but the K2+P2 was not as steep for the larger sizes and almost flat. The combinations with N2 had penetration curves that did not match any of the curves of the single mask. There are some hints that the bottom mask worn dictates the penetration curve of the combination.

Chapter 5

MEASURES TO QUANTIFY LEAKAGE

This experimental work is published in Physics of Fluids as "Quantification of Face Seal Leakage Using Parallel Resistance Model" (Pushpawela et al., 2023).

5.1 Resistance of Leaks

We propose a model to describe the leakage that occurs in the masks based on parallel flow resistances model. For the tests conducted on the mannequin head, a certain amount of air leaks where gaps between the mask and the face occur in the nasal or cheek areas. The linear relation between flow rate and pressure drop mirrors Ohm's Law. The pressure drop can be associated with the voltage in Ohm's law. The flow rate can be associated with the current. The regression slope can be associated with the resistance.

$$V = I \times R \quad (5.1)$$

where V is the voltage, I is the current, and R is the resistance as seen in Ohm's law here.

$$\Delta p = m \times Q \quad (5.2)$$

where Δp is the pressure drop, m is the regression slope, Q is the flow rate.

During inhalation, air may pass through the mask and be filtered, or it may leak through these lower pressure drop gaps that allow particles to escape filtration. The air that enters the mouth or nose is a mix of the filtered and unfiltered air flows. The system can be modelled as parallel resistances as shown in Figure 5.1. The material test's regression slope is solely for resistance associated with going through the mask without any leaks. The mannequin test's regression slope can be modelled as a parallel resistance, with one resistance being associated with going through the mask without any leaks, and the other resistance being associated with leaks at the nasal or cheek areas.

$$m_{mannequin} = \frac{R_1 \times R_2}{R_1 + R_2} \quad (5.3)$$

where $m_{mannequin}$ is the regression slope for the mannequin test, R_1 is the resistance of going through the mask without any leaks, and R_2 is the resistance of the leaks.

With the mathematical methodology explained above, the resistance of the leaks of various masks was found and shown in Table 5.1. For all of the masks, the

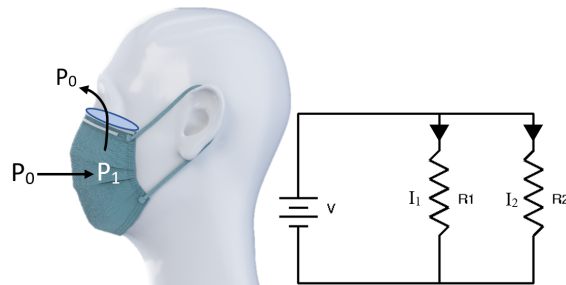


Figure 5.1: A drawing of the leaks on mask during inhalation (left). A circuit equivalent of our system (right).

| Mask | R_1 (Pa/LPM) | R_2 (Pa/LPM) |
|------|----------------|----------------|
| N1 | 0.7323 | 0.6775 |
| K1 | 1.301 | 1.186 |
| P1 | 0.4932 | 0.4154 |
| C1 | 0.8039 | 0.6359 |

Table 5.1: Resistance values without leaks (R_1) and with leaks (R_2).

resistance of flow through leaks is lower than that of going into the mouth. This can be attributed to the fact that a higher resistance would lead to a lower pressure inside the mask (P_1). The lower resistance of the gap will allow a high flow rate through the gap. The procedure masks have the least resistance through the mask and leaks and the KN95 respirators have the highest resistance for both categories. The leak resistance for KN95 and N95 respirators is higher because these two masks fit better to the face than the procedure and cloth masks. KN95 and N95 respirators typically have a metal bar at the nasal area in order to adjust for different nose shapes and less cheek area leakage than procedure and cloth masks. The resistance through the mask was simply due to the pressure drop associated with the mask because R_1 is just the slope of the flow rate and pressure drop graph. The KN95 respirator with the highest resistance had the highest pressure drop, and the procedure mask had the least resistance had the lowest pressure drop.

5.2 Flow Rate of Leaks

Since our material tests give us the pressure drop through the mask as a function of the total flow rate and we control the total air flow being "inhaled," the flow rate of the leaks can also be calculated from the data we have acquired. The difference between the through mask flow rate and the total flow is the leak flow rate. Leakage reduces the pressure drop that is observed in mannequin tests below that required

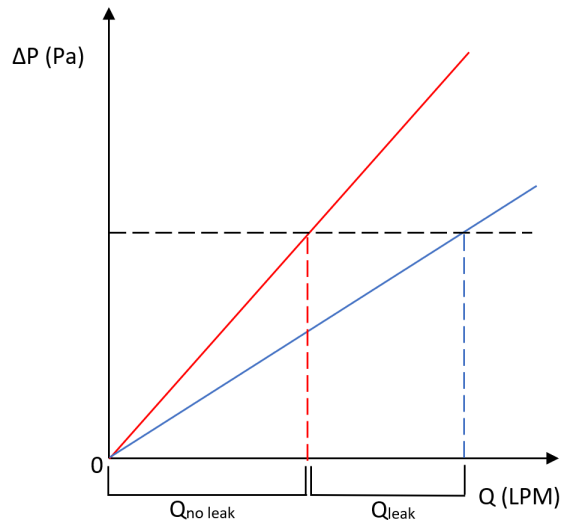


Figure 5.2: Sample graph of material and mannequin regression lines to show how the flow rate of leaks is found.

for the same total flow rate in the material tests. An illustration of the process to find the flow rate of the leaks is shown in Figure 5.2. The red line is representing the regression line for the material test. The blue line is representing the regression line for the mannequin test. For a specific flow rate, the pressure drop is some value for the material test indicated by the black horizontal dashed line that is found by multiplying the flow rate by the regression slope. This can be done for all the flow rates that have been tested. Then, with this pressure value, the flow rate in the mannequin test that corresponds to this pressure can be found by dividing the pressure value by the regression slope of the mannequin tests (blue line). The difference in the flow rate of the mannequin test and the original flow rate that was evaluated for the material test corresponds to the flow rate of the leakage.

To find the leakage flow rate, the pressure drops values for the material and mannequin tests must be evaluated. First of all, the pressure drop values found in the mannequin tests are lower than those found in the material tests for all flow rates. The difference in pressure drop between mannequin and material tests for N95 and KN95 respirators are less than those found in procedure and cloth mask. This can be linked to the better fit of the N95 and KN95 respirators than the procedure and cloth masks. Both procedure and cloth masks also tend to have noticeable gaps in the cheek areas, which the N95 and KN95 respirators do not have. Several publications have also investigated the pressure drop difference for procedure masks with leakage for NaCl aerosols, but in their studies, artificial leaks were utilized. At 30 LPM for

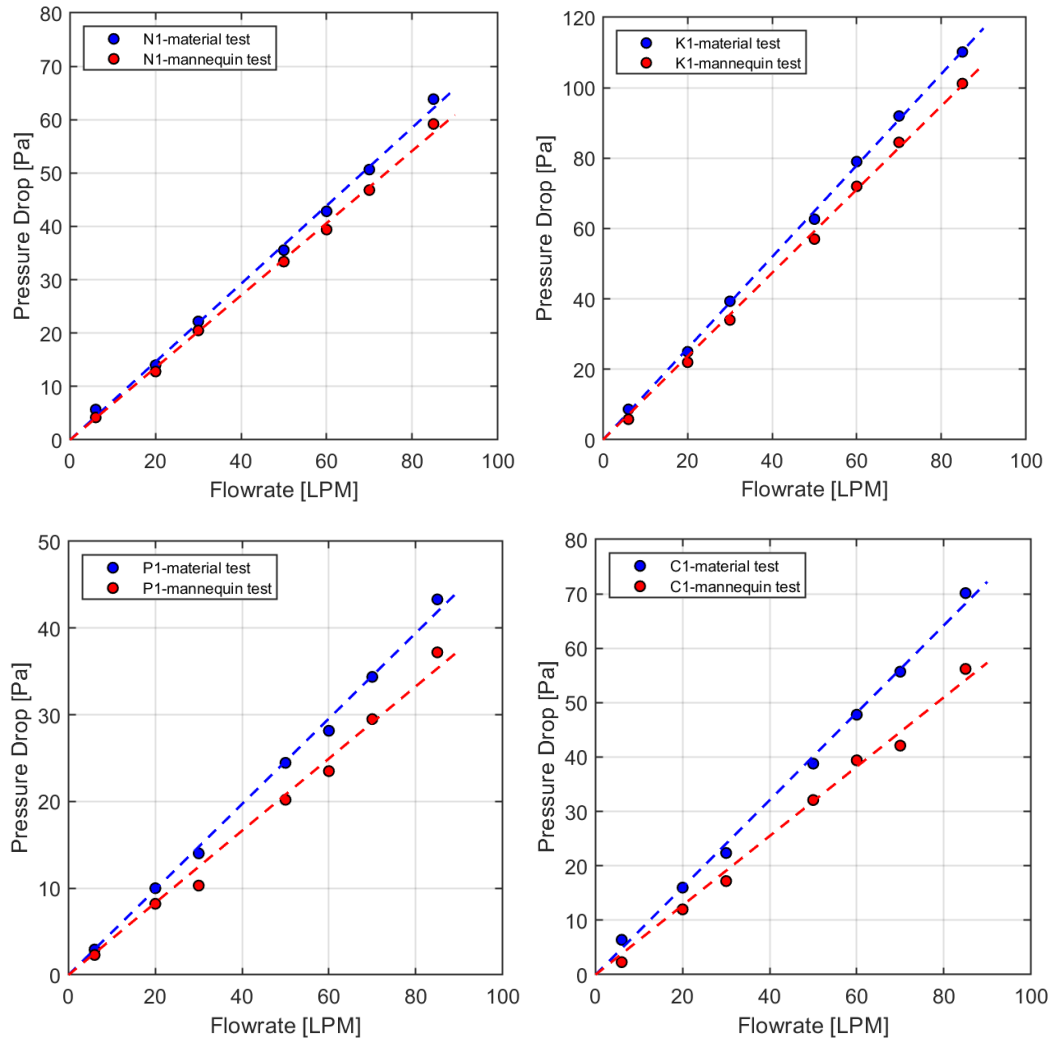


Figure 5.3: Pressure drop values for material and mannequin tests for different masks: N1 (top left), K1 (top right), P1 (bottom left), C1 (bottom right) as a function of flow rate.

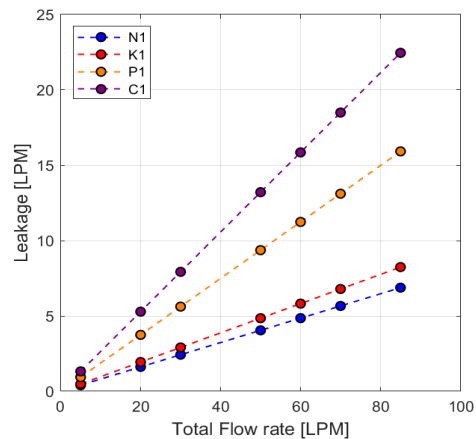


Figure 5.4: Graph of flow rate vs leakage flow rate.

a procedure mask, the pressure drop with no leaks was 17.7 Pa and with a 4mm diameter leak it was 16.6 Pa (Weber et al., 1993). In a different study, at 10 LPM for a procedure mask, the pressure drop with no leaks was 3.9 Pa and with two leaks of a diameter of 3 mm, it was 3.4 Pa (Guha et al., 2017). At 70 LPM for a procedure mask, the pressure drop with no leaks was 33 Pa and with leaks, it was 30 Pa. All of the pressure drop values in these studies, both with and without leaks, were higher than our observed values. In terms of pressure drop with leaks, our experiments utilized a "Fix the Mask" band to seal the KN95 respirator, procedure mask, and cloth mask, yielding a tight fit. The leakage area for this tight fit was not precisely measured, so it is hard to compare to the case with leaks in other studies mentioned along with the variation between masks that were utilized.

With the pressure drop values, the leakage flow rate can be found via the steps proposed earlier. The cloth mask has the highest leakage flow rate for all total flow rate values, and the N95 has the lowest leakage flow rate. For the cloth mask, the leakage flow rates were about 25% of the value of the total flow rates, which is quite a large proportion of the flow. This indicates that the design of the cloth masks tested does not ensure an adequate fit to the human face. In another study, two artificial leaks were punctured into the masks. For an N95 respirator, the total flow rate of 70 LPM has a leakage flow rate of 7.5 LPM, which is higher than our leakage flow rate of 5.7 LPM (Guha et al., 2017). For a procedure mask, the total flow rate of 70 LPM has a leakage flow rate of 9.6 LPM, which is less than our leakage flow rate of 13 LPM. The leaks had a diameter of 3 mm, and with their data being higher than ours may indicate that the area of our leakage is larger, which would allow the flow rate to be reduced.

Chapter 6

DISCUSSION AND FUTURE WORK

A major driving force for this research to investigate if wearing two masks is comparable to wearing one mask in terms of effectiveness with the given parameters measured. All double mask combinations had lower penetration values and higher pressure drops than wearing a corresponding single mask. There is a trade-off between penetration and pressure drop because a higher pressure drop indicates that less air is getting through the mask, which matches the meaning of lower penetration with a lower percentage of aerosol passing the mask. Higher pressure drop with wearing two masks is associated with lower breathability because more energy must be exerted to inhale and exhale. Because of this increased pressure drop, there has been some reluctance to wear multiple layers of masks, especially when people usually wear a single cloth or procedure mask, which have higher penetration values that can expose them to more aerosols, including ones with the SARS-CoV-2 virus.

The penetration of double mask combinations versus single mask brings up interesting trends and phenomena. The combination of masks that most of the public wear are cloth and procedure masks owing to their lower cost and higher supply compared to N95 and KN95 respirators. These respirators (especially N95) are saved for front line workers who deal with many more infected people than a common person would. Cloth masks can be used multiple times in contrast to electret respirators that lose their effectiveness more dramatically after the first use. In fact, the CDC recommends wearing two masks to improve the protection of the face covering (<https://www.cdc.gov/coronavirus/2019-ncov/your-health/effective-masks.html>). The penetration curves of both combinations of cloth and procedure masks have a similar shape to a single N95 respirator under the experimental condition that all masks were fully sealed. The MPPS of the N95 respirator was 80 nm, which was similar to the MPPS observed for both combinations. The maximum penetration for the N95 respirator and both combinations of cloth and procedure masks were all about 5%. However, both combinations had lower maximum penetration percentages than a single KN95 respirator (K2) that double mask testing was conducted for. Yet, a KN95 respirator (K1) had a similar peak penetration to both combinations. These data prove that wearing combinations of cloth and procedure masks are similar to wearing an N95 respirator and better than

a KN95 respirator in terms of maximum penetration. In terms of pressure drop, the combinations of cloth and procedure masks were greater than a single KN95 respirator, but less than all combinations involving KN95 and N95 respirators. Wearing a combination of cloth and procedure masks tightly significantly decreases in penetration compared to a single respective mask yet a slight increase in pressure drop compared to wearing a single KN95 respirator that has the highest pressure drop out of all of the single masks evaluated, yielding a practical balance between the two measures of the effectiveness of masks. In order to achieve similar performance that are reported here, people must wear double masks tightly with a good fit because our results are for a tightly sealed scenario.

The effects of penetration of combinations involving N95 and KN95 respirators was examined. All combinations involving these two respirators have a lower penetration compared to a single respirator. The peak penetration of around 2% for combinations with N95 respirators was about 50% than that of one N95 respirator (4.8%). The MPPS of the combinations was higher than an N95 respirator. For the KN95 respirator, the penetration decreased by 50% over portions of the size range for the combinations with KN95 respirators compared to a single KN95 respirator. The peak penetration was around 3% for combinations compared to 8% for a KN95 respirator. The pressure drop for combinations involving N95 and KN95 respirators was much higher than the KN95 respirator, which had the highest pressure drop out of all single masks. For the KN95 and N95 respirators, the slight decrease in peak penetration for combinations compared to single respirators does not seem practical for the dramatic increase in pressure drop.

This study looked into the effect of flow rates on penetration and pressure drop for single masks. We evaluated both measures at flow rates of 5, 30, and 85 LPM. 5 LPM represents a resting breathing rate. 30 LPM corresponds to a breathing rate while performing light exercise, and 85 LPM corresponds to a breathing rate while performing heavy exercise (Bałazy, Toivola, Reponen, et al., 2006). Pressure drop increased with increasing flow rate for all masks as reported in other papers (Guha et al., 2015; Jung et al., 2014). The KN95 respirator had the highest pressure drop, while the procedure mask had the lowest pressure drop. This indicates that the procedure mask has the highest breathability out of all masks tested. The N95 respirator and cloth mask have similar pressure drops over all flow rates, which could be due to a similar thickness of the mask material. Penetration increased with increasing flow rate for all masks and has been seen in other papers (Bałazy,

Toivola, Reponen, et al., 2006; Eninger et al., 2008; Guha et al., 2015). Comparing all of the masks, the peak penetration is lowest for N95 respirators at all flow rates, and the peak penetration is highest for cloth masks at all flow rates. A higher flow rate (inhalation breathing rate) causes increased pressure drop as well as increased penetration, which could increase the exposure of viral aerosol while lowering breathability.

The effects of leakage concerning mask performance were evaluated in this study. We observed that the resistance of air flow through leaks was smaller than going through the mask for all masks tested. Having a higher resistance to leaks indicates that it is harder for particles to escape through leaks for varying flow rates, which is a good feature for masks to possess. In addition, through comparing pressure drop data from material and mannequin tests, the leakage flow rates were found. Having a higher leakage flow rate means that more air flow is escaping the mask when inhaling. This could potentially either increase or decrease the amount of viral aerosol that is inhaled. There could be a varying amount of viral aerosol in the air that is leaked through the mask, which in turn impacts the probability of breathing in viral aerosol and other aerosols for that matter. The leakage flow rate should be reduced since when the exhalation case is considered, more leakages will occur that were not evaluated in this study. The cloth mask had the highest leakage flow rate across all total flow rates and the second lowest resistance for leaks. The procedure mask had the second highest leakage flow rate and lowest resistance for leaks. The two respirators tested had higher resistance values and lower leakage flow rates compared to the procedure and cloth masks. In addition, the penetration through leakage was higher in a procedure mask than an N95 respirator (Grinshpun et al., 2009). The procedure and cloth masks are more susceptible to leaks than respirators and thus reducing the effectiveness of procedure and cloth masks. This weakness could be remedied via wearing two masks as explained above or using a mask brace to improve fit.

Some aspects of mask performance that this research did not address would be potential directions for future work. One area is testing mask performance metrics over the different areas of the mask. Some masks tested in this study have different structural features that may have affected our data. Some examples are the cone and circular parts of the N95 respirator, the middle fold of the KN95 respirator, and the folds that occur in the procedure mask if not folded out completely. Another area is evaluating characteristics of leakage for exhalation. The reason is that the effects

of leakage are more noticeable when exhaling rather than inhaling. When exhaling, the mask is lifted from the face slightly, leading to potential viral particles being dispersed into the ambient air. The leakage areas of the nasal and cheeks are bigger when exhaling compared to inhaling. All of the studies utilized in this paper only tested leakage for inhalation (Grinshpun et al., 2009; He et al., 2014; Rengasamy et al., 2014). An additional area is to gain understanding about the penetration and pressure drop of double mask. There are analytical models for penetration and pressure drop of single mask. Developing an analytical framework for the measures of effectiveness for double mask could be an interesting research direction. Few papers have been published about double masks, so there is not little data with which to compare our data. The last area is to develop a model to effectively predict mask performance for the general public. There are equations that model pressure drop and penetration well as seen in (Huang et al., 2013). However, it is hard for a member of the general public to easily understand the variables that are needed to utilize these equations. Perhaps a simple and portable apparatus could be built in order to test mask performance metrics. An optical particle counter which is more cost-effective compared to our experimental equipment could be used.

BIBLIOGRAPHY

- Bařazy, A., Toivola, M., Adhikari, A., Sivasubramani, S. K., Reponen, T., & Grinshpun, S. A. (2006). Do n95 respirators provide 95% protection level against airborne viruses, and how adequate are surgical masks? *American journal of infection control*, 34(2), 51–57.
- Bařazy, A., Toivola, M., Reponen, T., Podgórski, A., Zimmer, A., & Grinshpun, S. A. (2006). Manikin-based performance evaluation of n95 filtering-facepiece respirators challenged with nanoparticles. *Annals of Occupational Hygiene*, 50(3), 259–269.
- Brochot, C., Saidi, M. N., & Bahloul, A. (2020). How Effective Is the Filtration of ‘KN95’ Filtering Facepiece Respirators During the COVID-19 Pandemic? [wxaa101]. *Annals of Work Exposures and Health*. <https://doi.org/10.1093/annweh/wxaa101>
- Brooks, J. T., Beezhold, D. H., Noti, J. D., Coyle, J. P., Derk, R. C., Blachere, F. M., & Lindsley, W. G. (2021). Maximizing fit for cloth and medical procedure masks to improve performance and reduce sars-cov-2 transmission and exposure, 2021. *Morbidity and Mortality Weekly Report*, 70(7), 254.
- Chia, P. Y., Coleman, K. K., Tan, Y. K., Ong, S. W. X., Gum, M., Lau, S. K., Sutjipto, S., Lee, P. H., Young, B. E., Milton, D. K., et al. (2020). Detection of air and surface contamination by severe acute respiratory syndrome coronavirus 2 (sars-cov-2) in hospital rooms of infected patients. *MedRxiv*.
- Cho, H.-w., Yoon, C.-S., Lee, J.-H., Lee, S.-j., Viner, A., & Johnson, E. W. (2011). Comparison of pressure drop and filtration efficiency of particulate respirators using welding fumes and sodium chloride. *Annals of occupational hygiene*, 55(6), 666–680.
- Clapp, P. W., Sickbert-Bennett, E. E., Samet, J. M., Berntsen, J., Zeman, K. L., Anderson, D. J., Weber, D. J., Bennett, W. D., et al. (2020). Evaluation of cloth masks and modified procedure masks as personal protective equipment for the public during the covid-19 pandemic. *JAMA internal medicine*.
- Crilley, L., Malile, B., Angelucci, A., Young, C., VandenBoer, T. C., Jennifer, I., & Chen, L. (2021). Non-woven materials for cloth-based face mask inserts: Relationship between material properties and sub-micron aerosol filtration. *Environmental Science: Nano*.
- Eninger, R. M., Honda, T., Adhikari, A., Heinonen-Tanski, H., Reponen, T., & Grinshpun, S. A. (2008). Filter performance of n99 and n95 facepiece respirators against viruses and ultrafine particles. *Annals of occupational hygiene*, 52(5), 385–396.

- Fears, A., Klimstra, W., Duprex, P., Hartman, A., Weaver, S., Plante, K., Mirchandani, D., Plante, J., Aguilar, P., Fernández, D., Nalca, A., Totura, A., Dyer, D., Kearney, B., Lackemeyer, M., Bohannon, J., Johnson, R., Garry, R., Reed, D., & Roy, C. (2020). Comparative dynamic aerosol efficiencies of three emergent coronaviruses and the unusual persistence of sars-cov-2 in aerosol suspensions. *medRxiv*. <https://doi.org/10.1101/2020.04.13.20063784>
- Gandhi, M., & Marr, L. C. (2021). Uniting infectious disease and physical science principles on the importance of face masks for covid-19. *Med*, 2(1), 29–32.
- Gao, S., Kim, J., Yermakov, M., Elmashae, Y., He, X., Reponen, T., Zhuang, Z., Rengasamy, S., & Grinshpun, S. A. (2016). Performance of n95 ffrs against combustion and nacl aerosols in dry and moderately humid air: Manikin-based study. *Annals Of Occupational Hygiene*, 60(6), 748–760.
- Grinshpun, S. A., Haruta, H., Eninger, R. M., Reponen, T., McKay, R. T., & Lee, S.-A. (2009). Performance of an n95 filtering facepiece particulate respirator and a surgical mask during human breathing: Two pathways for particle penetration. *Journal of occupational and environmental hygiene*, 6(10), 593–603.
- Guha, S., McCaffrey, B., Hariharan, P., & Myers, M. R. (2017). Quantification of leakage of sub-micron aerosols through surgical masks and facemasks for pediatric use. *Journal of occupational and environmental hygiene*, 14(3), 214–223.
- Guha, S., Mejía-Alfaro, A., Hariharan, P., & Myers, M. R. (2015). Effectiveness of facemasks for pediatric populations against submicron-sized aerosols. *American journal of infection control*, 43(8), 871–877.
- Hao, J., Passos de Oliveira Santos, R., & Rutledge, G. C. (2021). Examination of nanoparticle filtration by filtering facepiece respirators during the covid-19 pandemic. *ACS Applied Nano Materials*. <https://doi.org/10.1021/acsnm.1c00139>
- He, X., Grinshpun, S. A., Reponen, T., McKay, R., Bergman, M. S., & Zhuang, Z. (2014). Effects of breathing frequency and flow rate on the total inward leakage of an elastomeric half-mask donned on an advanced manikin headform. *Annals of occupational hygiene*, 58(2), 182–194.
- Hering, S. V., Lewis, G. S., Spielman, S. R., & Eiguren-Fernandez, A. (2019). A magic concept for self-sustained, water-based, ultrafine particle counting. *Aerosol Science and Technology*, 53(1), 63–72.
- Hering, S. V., Spielman, S. R., & Lewis, G. S. (2014). Moderated, water-based, condensational particle growth in a laminar flow. *Aerosol Science and Technology*, 48(4), 401–408.
- Huang, S.-H., Chen, C.-W., Chang, C.-P., Lai, C.-Y., & Chen, C.-C. (2007). Penetration of 4.5 nm to 10um aerosol particles through fibrous filters. *Journal of Aerosol Science*, 38(7), 719–727.

- Huang, S.-H., Chen, C.-W., Kuo, Y.-M., Lai, C.-Y., McKay, R., Chen, C.-C., et al. (2013). Factors affecting filter penetration and quality factor of particulate respirators. *Aerosol and Air Quality Research*, *13*(1), 162–171.
- Jung, H., Kim, J. K., Lee, S., Lee, J., Kim, J., Tsai, P., Yoon, C., et al. (2014). Comparison of filtration efficiency and pressure drop in anti-yellow sand masks, quarantine masks, medical masks, general masks, and handkerchiefs. *Aerosol and Air Quality Research*, *14*(3), 991–1002.
- Lednicky, J. A., Lauzardo, M., Fan, Z. H., Jutla, A., Tilly, T. B., Gangwar, M., Usmani, M., Shankar, S. N., Mohamed, K., Eiguren-Fernandez, A., Stephenson, C. J., Alam, M. M., Elbadry, M. A., Loeb, J. C., Subramaniam, K., Waltzek, T. B., Cherabuddi, K., Morris, J. G., & Wu, C.-Y. (2020). Viable sars-cov-2 in the air of a hospital room with covid-19 patients. *International Journal of Infectious Diseases*, *100*, 476–482. <https://doi.org/https://doi.org/10.1016/j.ijid.2020.09.025>
- Li, Y., Qian, H., Hang, J., Chen, X., Hong, L., Liang, P., Li, J., Xiao, S., Wei, J., Liu, L., & Kang, M. (2020). Evidence for probable aerosol transmission of sars-cov-2 in a poorly ventilated restaurant. *medRxiv*. <https://doi.org/10.1101/2020.04.16.20067728>
- Liu, C., Mendonça, L., Yang, Y., Gao, Y., Shen, C., Liu, J., Ni, T., Ju, B., Liu, C., Tang, X., et al. (2020). The architecture of inactivated sars-cov-2 with postfusion spikes revealed by cryo-em and cryo-et. *Structure*, *28*(11), 1218–1224.
- Ma, J., Qi, X., Chen, H., Li, X., Zhang, Z., Wang, H., Sun, L., Zhang, L., Guo, J., Morawska, L., Grinshpun, S., Biswas, P., Flagan, R., & Yao, M. (2020). Exhaled breath is a significant source of sars-cov-2 emission. <https://doi.org/10.1101/2020.05.31.20115154>
- Miller, S. L., Nazaroff, W. W., Jimenez, J. L., Boerstra, A., Buonanno, G., Dancer, S. J., Kurnitski, J., Marr, L. C., Morawska, L., & Noakes, C. (2021). Transmission of sars-cov-2 by inhalation of respiratory aerosol in the skagit valley chorale superspreading event. *Indoor Air*, *31*(2), 314–323. <https://doi.org/https://doi.org/10.1111/ina.12751>
- Moore, G., Rickard, H., Stevenson, D., Bou, P. A., Pitman, J., Crook, A., Davies, K., Spencer, A., Burton, C., Easterbrook, L., Love, H. E., Summers, S., Welch, S. R., Wand, N., Thompson, K.-A., Pottage, T., Richards, K. S., Dunning, J., & Bennett, A. (2020). Detection of sars-cov-2 within the healthcare environment: A multicentre study conducted during the first wave of the covid-19 outbreak in england. *Journal of Hospital Infection*. <https://doi.org/10.1016/j.jhin.2020.11.024>
- Morawska, L., Tang, J. W., Bahnfleth, W., Bluyssen, P. M., Boerstra, A., Buonanno, G., Cao, J., Dancer, S., Floto, A., Franchimon, F., Haworth, C., Hogeling, J., Isaxon, C., Jimenez, J. L., Kurnitski, J., Li, Y., Loomans, M., Marks,

- G., Marr, L. C., ... Yao, M. (2020). How can airborne transmission of covid-19 indoors be minimised? *Environment International*, *142*, 105832. <https://doi.org/https://doi.org/10.1016/j.envint.2020.105832>
- Pan, J., Harb, C., Leng, W., & Marr, L. C. (2021). Inward and outward effectiveness of cloth masks, a surgical mask, and a face shield. *Aerosol Science and Technology*, 1–17.
- Rengasamy, S., Eimer, B. C., & Shaffer, R. E. (2009). Comparison of nanoparticle filtration performance of niosh-approved and ce-marked particulate filtering facepiece respirators. *Annals of Occupational Hygiene*, *53*(2), 117–128.
- Rengasamy, S., Eimer, B. C., & Szalajda, J. (2014). A quantitative assessment of the total inward leakage of nacl aerosol representing submicron-size bioaerosol through n95 filtering facepiece respirators and surgical masks. *Journal of occupational and environmental hygiene*, *11*(6), 388–396.
- Sheets, D., Shaw, J., Baldwin, M., Daggett, D., Elali, I., Curry, E. B., Sochnikov, I., & Hancock, J. N. (2020). An apparatus for rapid and nondestructive comparison of masks and respirators. *Review of Scientific Instruments*, *91*(11), 114101.
- Sickbert-Bennett, E. E., Samet, J. M., Clapp, P. W., Chen, H., Berntsen, J., Zeman, K. L., Tong, H., Weber, D. J., & Bennett, W. D. (2020). Filtration efficiency of hospital face mask alternatives available for use during the covid-19 pandemic. *JAMA Internal Medicine*, *180*(12), 1607–1612. <https://doi.org/10.1001/jamainternmed.2020.4221>
- Ueki, H., Furusawa, Y., Iwatsuki-Horimoto, K., Imai, M., Kabata, H., Nishimura, H., & Kawaoka, Y. (2020). Effectiveness of face masks in preventing airborne transmission of sars-cov-2. *MSphere*, *5*(5).
- van Doremalen, N., Bushmaker, T., Morris, D. H., Holbrook, M. G., Gamble, A., Williamson, B. N., Tamin, A., Harcourt, J. L., Thornburg, N. J., Gerber, S. I., Lloyd-Smith, J. O., de Wit, E., & Munster, V. J. (2020). Aerosol and surface stability of sars-cov-2 as compared with sars-cov-1. *New England Journal of Medicine*, *382*(16), 1564–1567. <https://doi.org/10.1056/NEJMc2004973>
- van der Vossen, J. M., Heerikhuisen, M., Traversari, R. A., van Wuijckhuijse, A. L., & Montijn, R. C. (2021). Heat sterilization dramatically reduces filter efficiency of the majority of ffp2 and kn95 respirators. *Journal of Hospital Infection*, *107*, 87–90.
- Weber, A., Willeke, K., Marchloni, R., Myojo, T., Mckay, R., Donnelly, J., & Liebhauer, F. (1993). Aerosol penetration and leakae characteristics of masks used in the health care industry. *American journal of infection control*, *21*(4), 167–173.
- Wen, Z., Yu, L., Yang, W., Hu, L., Li, N., Wang, J., Li, J., Lu, J., Dong, X., Yin, Z., et al. (2013). Assessment the protection performance of different level personal respiratory protection masks against viral aerosol. *Aerobiologia*, *29*(3), 365–372.

Xie, X., Li, Y., Chwang, A. T., Ho, P.-L., & Szeto, W.-H. (2007). How far droplets can move in indoor environments – revisiting the wells evaporation–falling curve. *Indoor Air*, *17*(3), 211–225. <https://doi.org/https://doi.org/10.1111/j.1600-0668.2007.00469.x>

Appendix A

SPECIFICATION OF MASKS

Table A.1: Specification of masks.

| Sample | Specifications | Manufacturer/Distributor |
|--|---|---|
| NIOSH-certified N95 respirators | | |
| N1 | 3M 8210, head loops, TC-B4A-007, Lot# A20091 | 3M, USA |
| N2 | SH 9550, head loops, TC-84A-3713, UNIAIR | San Huei United Company Ltd, Taiwan / Caltech Stockroom |
| KN95 respirators | | |
| K1 | GB 2626-2006 standard, ear loops | Zhejiang Rex Intelligent Technology Ltd, China / BBCraft.com |
| K2 | GB 2626-2006 standard, ear loops, 45% non-woven fabric, 25% electrostatic filtration cotton, 30% melt-blown fabric | Guangdong Marbon Daily & Chemical Ltd, China / Honest PPE Supply (Well Before) |
| Procedure masks | | |
| P1 | Ear loops | Human Health Organization / B&D imports |
| P2 | Ear loops, 66% non-woven fabric, 34% melt-blown fabric | Guangdong Marbon Daily & Chemical Ltd, China / Honest PPE Supply (Well Before) |
| Cloth masks | | |
| C1 | Ear loops, 3 layers, 95% cotton, 5% poly-cotton blend | Sock Fancy / Caltech Book Store |
| C2 | Ear loops | Guangzhou City Baiyun District Etai Garment Factory, China / Honest PPE Supply (Well Before) |

Appendix B

LINEAR PLOTS OF PENETRATION FOR DOUBLE MASKS

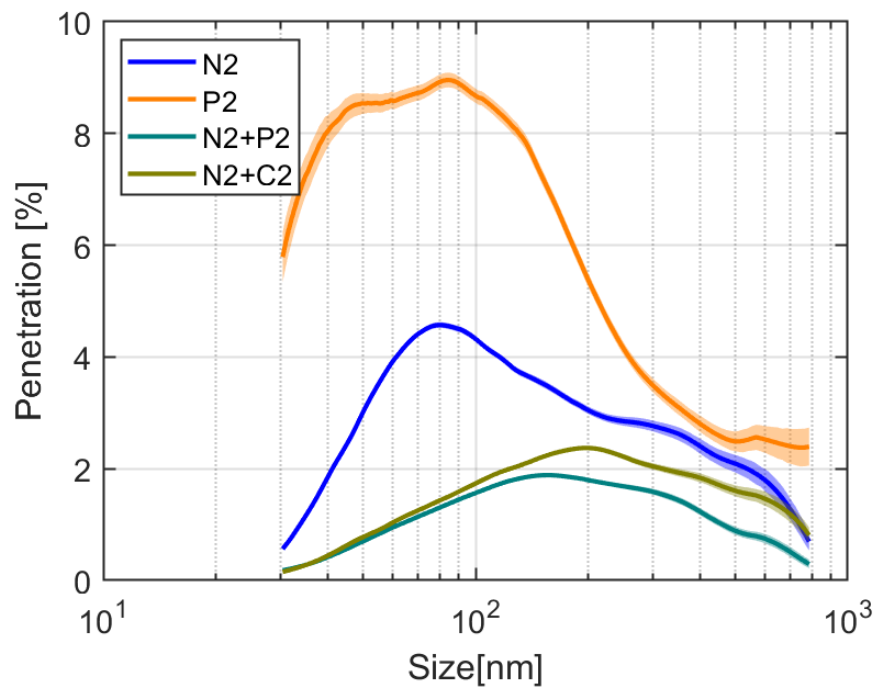


Figure B.1: Linear plot of penetration of N2 with different masks worn on top of it.

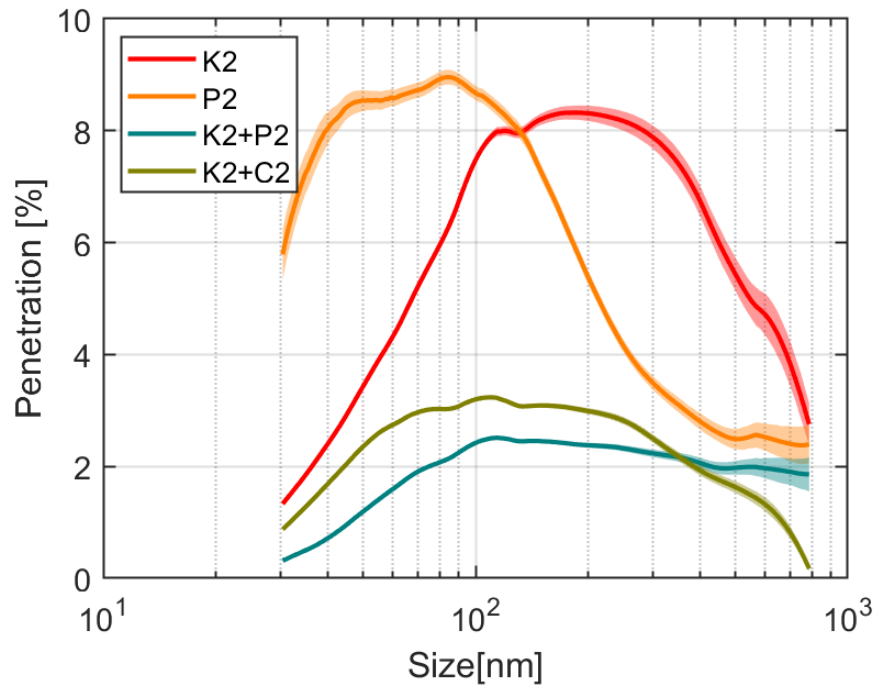


Figure B.2: Linear plot of penetration of K2 with different masks worn on top of it.

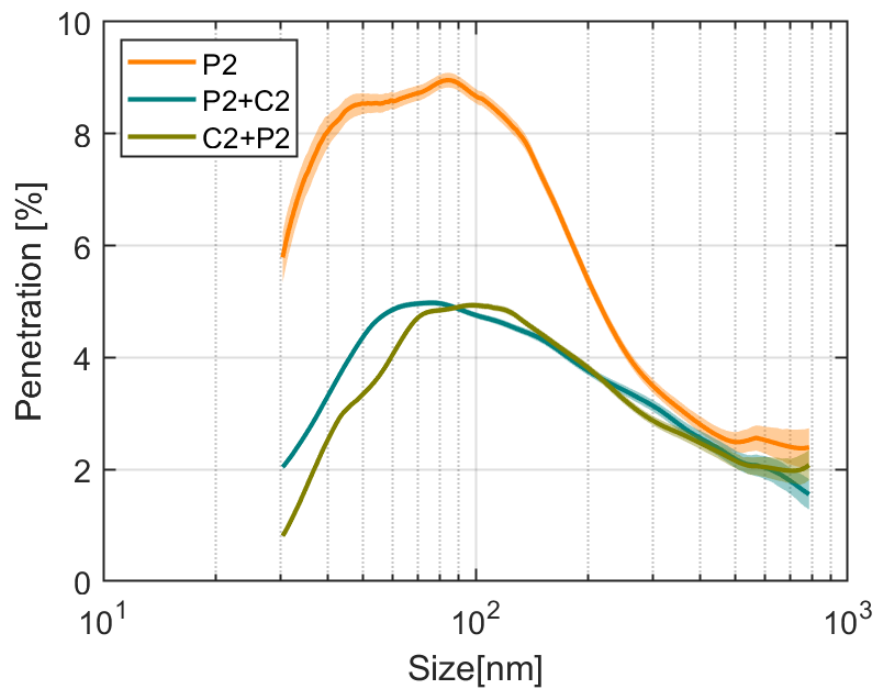


Figure B.3: Linear plot of penetration of P2 with different masks worn on top of it.

Appendix C

UPDATES TO THIS THESIS IN 2024

The main body (Chapters 1-6 and Abstract) along with Appendices A, B, and D were primarily written in 2021 with some edits in 2022.

During the period between 2022-2024, I was working along with the co-authors to publish two papers that included experimental work conducted during this thesis. The two publications are listed in the "Published Content and Contributions" section. Additionally, two abstracts were accepted as platform presentations for the 2024 American Association for Aerosol Research (AAAR) Annual Conference in Albuquerque, New Mexico.

When I was writing this thesis in 2021, I genuinely thought that I was going to continue be in the air quality field. So, I applied for master's programs in environmental science in 2022. But then, Professor Mark Davis mentioned that he was starting a company to commercialize green hydrogen production via a thermochemical water splitting cycle. I started with HGenium in July 2022 and I truly have grown further as an independent researcher. The moral of my budding career is that life is unpredictable.

Appendix D

ABSTRACT SUBMITTED FOR AAAR 2021 CONFERENCE

Some portions of this research were submitted and chosen as an abstract in the category of "Infectious Aerosols in the Age of COVID-19." I presented this research at the 2021 American Association for Aerosol Research (AAAR) Annual Conference in Albuquerque, New Mexico (virtual). The abstract is titled "Influence of Flow Rates on Pressure Drop and Penetration for Various Masks." The authors listed on the abstract are Peter Chea, Buddhi Pushpawela, Ryan Ward, and Richard Flagan. The abstract in its entirety is presented below.

Mask-wearing emerged as the primary safety measure to prevent spreading COVID-19. To assess the viability of different materials in filtering aerosols when inhaling, we tested multiple copies of different mask categories: including NIOSH-certified N95 respirators, KN95 masks, procedure masks, and cloth masks. The intact masks were exposed to polydisperse NaCl aerosol of 30-800 nm, and tightly sealed within a chamber to get the upstream and downstream particle counts and pressure measurements. The pressure drop was measured for seven flow rates between 5 and 85 LPM. For all masks, it increased linearly with flow rate with $r^2 > 0.98$. The KN95 and cloth masks had higher pressure drops than the other masks, causing reduced breathability. The penetration was calculated with counts from a differential mobility analyzer and condensation particle counter system for three flow rates: 5, 30, and 85 LPM. For all of the masks, the penetration increased with flow rate, while the most penetrating particle size (MPPS) generally decreased. However, N95 and KN95 electret masks did not exhibit a significant shift in MPPS when the flow rate increased from 5 to 85 LPM. Compared to electret masks, the shift in MPPS for procedure and cloth masks was significant. This behavior shows that, for increased flow rates, the effectiveness of diffusion and electrostatic attraction (mainly affecting small particles) decreases, while that of impaction (mainly affecting large particles) increases. The use of face masks at high flow rates increases the risk to the wearer, and reduces breathability. The reduction of breathability may cause the public to be hesitant to wear masks.

*Appendix E***ABSTRACTS SUBMITTED FOR AAAR 2024 CONFERENCE**

The work about double masking was submitted and was accepted for the 2024 AAAR Annual Conference in Albuquerque, New Mexico. The abstract is titled "The Potential Efficacy of Double Masking." The authors listed on the abstract are Peter Chea, Buddhi Pushpawela, Ryan Ward, and Richard Flagan. The abstract in its entirety is presented below.

Double masking generally decreases the penetration of particles and increases the pressure drop compared to the individual mask. When we wear the two masks the outer mask provides pressure to the edges of the inner mask, and therefore the inner mask fits more closely to the face and creates a better seal and an additional layer of protection. During the COVID-19 pandemic, the Centers for Disease Control and Prevention (CDC) and health experts recommended double masking to improve protection. However, the performance of double masks related to their particle penetration, pressure drops (breathing resistance or comfort), type of the masks, and combinations was limited in the literature. To address these limitations, we measured and compared the particle penetration and pressure drop of single and double masks (6 different combinations) that were fully sealed at a steady flow rate of 30 LPM. Of the double masks tested, N95 + procedure masks, N95 + cloth masks, KN95 + procedure masks, KN95 + cloth masks, and procedure + cloth masks showed 3-5% penetration, comparable with that of the N95s. The pressure drop measured for different double mask combinations varied between 38 and 83 Pa. These pressure drop values agreed well with the theoretical pressure drops estimated by the sum of the respective pressure drop values of single masks. The combination of procedure and cloth masks had similar pressure drops and penetration performance to a single respirator, making this double mask combination adequate in situations where respirators are less cost-effective or in limited supply. Therefore, the results of this study offer information to the community about the proper mask combinations that provide more protection than the individual mask.

The work about leakage of masks was submitted and was accepted for the 2024 AAAR Annual Conference in Albuquerque, New Mexico. The abstract is titled "The Potential Efficacy of Double Masking." The authors listed on the abstract are Buddhi Pushpawela, Peter Chea, Ryan Ward, and Richard Flagan. The abstract in its entirety is presented below.

Masks and respirators afford varying degrees of protection to the person wearing them. The degree of protection depends upon the material (filter medium), the design and construction of the masks, manufacture, fit of the mask (how well it seals to the face), the nature of the particles that carry the virus, the respiration rate, as well as the percentage of particles penetrating through the face seal leakage, the total flow rate through the filter medium and other factors. Therefore, identifying the leaking places of masks and quantifying the leakage flow rate is important to estimate the protection.

In our study, we hypothesized a model to quantify the leakage flow rate through the face mask based on a parallel resistance model. We used Ohm's law as an analogy for the pressure leakage rate. The tests were performed in two ways; (i) mask material test, in which all masks were sealed to a flange to measure transmission through a full mask and prevent leakage around the edges (ii) mannequin mask test, in which masks are fitted to a mannequin head tightly. In this study, we have tested four different classes of masks: NIOSH-certified N95 Face Filtering Respirators (FFRs), KN95 masks, 3-ply, pleated, disposable procedure masks, and cloth masks. For all the FFRs and masks, the pressure drop was measured at eight different flow rates between 5 and 85 LPM, and it was increased linearly with the total flow rate ($r^2 > 0.98$). The results of the study showed that the leakage flow rate was 10% of the total flow rate, even for the best-fitted N95 FFRs and KN95 masks. They showed higher resistance to the leaks. The procedure masks and cloth masks showed a leakage flow rate of 25% of the value of the total flow rate, quite a large proportion of the flow. They had lower resistance to leaks. This parallel resistance model can help improve mask design and obtain better mask sealing.